Journal of Hazardous Materials 439 (2022) 129588

Contents lists available at ScienceDirect

Journal of Hazardous Materials

journal homepage: www.elsevier.com/locate/jhazmat

Research Paper

Cellulose and its derivatives, coffee grounds, and cross-linked, β-cyclodextrin in the race for the highest sorption capacity of cationic dyes in accordance with the principles of sustainable development

Anna Maria Skwierawska [a,*], Monika Bliźniewska [a], Kinga Muza [a], Agnieszka Nowak [a], Dominika Nowacka [a], Shan E. Zehra Syeda [a], Muhammad Shahzeb Khan [a], Bogusława Łęska [b]

[a] Department of Chemistry and Technology of Functional Materials, Faculty of Chemistry, Gdańsk University of Technology, 11/12 Narutowicza street, 80-233 Gdańsk, Poland
[b] Faculty of Chemistry, Adam Mickiewicz University, 8 Uniwersytetu Poznańskiego street, 61-614 Poznań, Poland

HIGHLIGHTS

- Natural or semi-natural sorption materials which are better?
- The reaction solvent shapes the sorption properties of the polymers.
- Pollutant shape memory as the basis for the stability of sorbent efficiency.
- Waste-free regeneration of adsorbents.
- Possible decomposition of used adsorbents by composting.

GRAPHICAL ABSTRACT

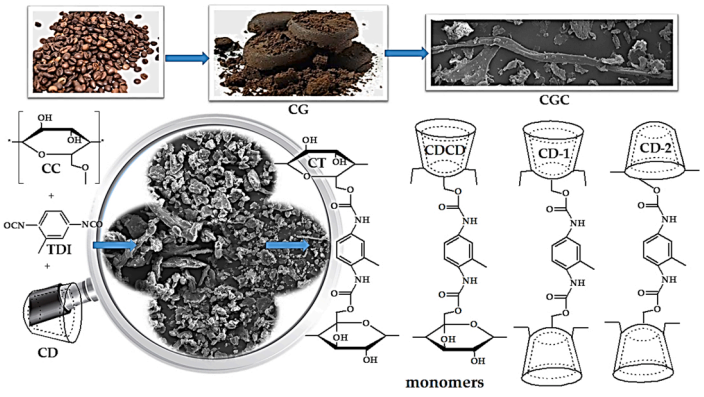

ARTICLE INFO

Editor: Arturo J Hernandez-Maldonado

Keywords:
Selective substitution
Hydrogen bonds
Supramolecular complex

ABSTRACT

In this study, seven different materials were analyzed and includes coffee grounds (CG), two types of cellulose (CGC and CC), two types of modified cellulose (CT and CTCD), and cross-linked β-cyclodextrin (CD-1 and CD-2) were tested as adsorbents for the removal of dyes from the wastewater. The composition, morphology, and presence of functional groups in the obtained sorption materials were characterized by elemental analysis, SEM, TG/DTA, and FTIR spectroscopy. The sorption processes of the model contaminant, crystal violet (CV), were

Abbreviations: BG, brilliant green; BP, bromocresol purple sodium salt; CC, cellulose microcrystalline; β-CD CD, β-cyclodextrin; CD-1, sorbent obtained in reaction of cyclodextrin with toluene-2,4-di-isocyanate conducted in a pyridine medium; CD-2, sorbent obtained in reaction of cyclodextrin with toluene-2,4-di-isocyanate conducted in a dimethylformamide medium; CG, coffee grounds; CR, Congo red; CT, cellulose sorbent obtained in reaction microcrystalline cellulose with toluene-2,4-di-isocyanate in a pyridine medium; CTCD, sorbent obtained in reaction of microcrystalline cellulose and cyclodextrin with toluene-2,4-di-isocyanate in a pyridine medium; CV, crystal violet; DMF, dimethylformamide; EB, eriochrome black; HA, a mixture of humic acids 50% fulvic acids; MB, methylene blue; TB, toluidine blue; TDI, Itoluene-2,4-di-isocyanate.

* Correspondence to: 11/12 Narutowicza street, 80-233 Gdańsk, Poland.
E-mail address: anna.skwierawska@pg.edu.pl (A.M. Skwierawska).

https://doi.org/10.1016/j.jhazmat.2022.129588
Received 16 March 2022; Received in revised form 6 July 2022; Accepted 10 July 2022
Available online 14 July 2022

Shape memory
Yeast

studied by kinetics and equilibrium models. The results showed, that using CTCD, the dye was adsorbed rapidly in 1 min and the slowest adsorption occurred in 20 min by CG. The time evolution was adjusted using a two-model, pseudo second-order model (CG and CGC) and pseudo first-order model in the rest adsorbents. According to the Langmuir and Sips isotherm models, the maximum adsorption capacities were very high in each case ranging from 1092.24 to 1220.40 mg g^{-1}. Moreover, the adsorption capacity of the near-natural materials remained even higher after five regeneration cycles. The regeneration is almost waste-free and the materials used can be decomposed during composting. In addition, almost complete removal of cationic dyes was observed during the treatment of real wastewater samples.

1. Introduction

1.1. Natural origin adsorbents

Currently, a lot of attention is being paid to organic adsorbents (Marincas et al., 2016), seeing the possibility of final degradation through biodegradation (Karoyo et al., 2018). These adsorbents can be divided into four groups. The first is chemically unmodified, it includes various types of plant waste such as shells (Bulut and Aydin, 2006; Ferrero, 2007; Queirós et al., 2020), skins (Trends et al., 2021), fruits (Harshananda et al., 2020; Sathishkumar et al., 2015), leaves and barks (Ayalew and Aragaw, 2020; Futalan et al., 2019; Ibiyinka et al., 2021; Kim and Kim, 2020; Oliveira et al., 2008; Pavan et al., 2008). However, completely crude form was quite difficult to use, the plant raw material was first grounded and dried to a constant weight, and physically processed to remove undesirable components. Thus, the group of adsorbents obtained in this way includes coffee grounds and tea leaves (Lafi et al., 2014; Loulidi et al., 2021), citrus and banana peels, and nut shells (Rafatullah et al., 2010). The nature-compatible form of the adsorbent enables biological decomposition at a rate appropriate for a given plant (Chalker-scott, 2021; Kalemelawa et al., 2012; Raimondo et al., 2018; Scroll and For, 2012). The second group consists of adsorbents obtained from the above-mentioned raw materials as a result of chemical or biotechnological reactions (Brinchi et al., 2013; Kim et al., 1997; Liu et al., 2016; Rajput et al., 2016; J. Zhang et al., 2019; Zhong, 2020). These are the main plant components, i.e. cellulose, hemicellulose, and lignin, but also chitin and cyclodextrin (Militao et al., 2021; Shahnaz et al., 2021). The third group consists of adsorbents containing components of natural origin incorporated into the structure of the material by means of chemical reactions (Ding et al., 2020; A.M. Elgarahy et al., 2019, 2021; Ahmed M. Elgarahy et al. 2019; Elwakeel, 2009; Elwakeel et al., 2021b, 2021a, 2020; Erdös et al., 2020; Soares et al., 2019; Yang et al., 2020). The last one consists of various types of carbons obtained during the pyrolysis of various natural resources (Tomul et al., 2020; Yi et al., 2019). To practice the principles of sustainable development during the preparation of the adsorbents, following should consider the reduction of energy consumption and emission of gases, waste, and sewage during its production, regeneration, and disposal, which were quite difficult to achieve. Therefore, the basic problem is to keep the technological moderation that allows obtaining the cost-effective adsorbent in the least number of preparatory steps, but with a high sorption capacity.

1.2. Dye adsorption

Dye was checked using simple devices for adsorption purposes in the wastewater. Due to the increase in anthropogenic activities, there is an exponential increase in dye contaminants around the world. Additionally, the production of dyes and dyeing processes are an example of an industry that generates a large amount of wastewater containing organic substances (Katheresan et al., 2018; Liu, 2020; Shindhal et al., 2021). Dyes are a real environmental threat because they are not biodegradable (Garg and Chopra, 2022; Lellis et al., 2019) and the colored sewage hinders the growth of microorganisms and plants responsible for phytoremediation of waters. In factories and dye works, various solutions are used to reduce the emission of dyes to the natural environment. The most frequently used methods to remediate dye pollutants from the environment are physical, chemical and biological (Dutta et al., 2021). None of the above-mentioned methods are fully effective; therefore, new solutions are constantly sought, including organic absorbents. Dyes are designed in a way that allows permanent interaction with the colored surface. In the case of cotton and modified cellulose fibers, where dyes are often used and bind with the material through hydrogen bonding and van der Waals forces. The weak interactions are compensated by the multitude of free hydroxyl groups present in the glucose monomers. An example of such dye is triarylmethane derivatives containing amino groups. Furthermore, using cellulose adsorbents is an effective approach to remove these dyes from wastewater, but the problem is regeneration, which uses too many extractions. A potential solution may be the use of β-cyclodextrin polymers that selectively interact with dyes of this group by inclusion of one of the rings inside the torus. Similarly, the resulting supramolecular complex can be easily broken down which makes the desorption process easier.

In this study, seven adsorbents were intentionally selected: spent coffee grounds (CG), cellulose obtained from coffee grounds (CGC), commercial microcrystalline cellulose (CC); and four materials derived from the condensation of toluene-2,4-diisocyanate with microcrystalline cellulose (CT); a mixture of microcrystalline cellulose and β-CD (CTCD) and β-CD alone (CD-1 and CD-2). From the comparison of the first two, it was expected to obtain a result indicating the validity of the production of technical cellulose used in the removal of dyes from the environment. The choice of microcrystalline cellulose was aimed at highlighting the structural differences with respect to CGC affecting the durability of the obtained connections and the resulting problems during regeneration. Moreover, the synthesis of CT and CTCD was also a deliberate procedure. First, the modification with toluene-2,4-diisocyanate changes the hydrophobicity of cellulose. Secondly, in the case of CT, a more ordered structure and a greater likelihood of the emergence of $\pi - \pi$ interactions were to be expected. The addition of β-CD to the system made it possible to determine the importance of selective interaction with a specific dye. Knowing the influence of β-CD on the sorption capacity of the two-component material, it was still necessary to determine the flow of the arrangement of groups acting as linkers.

2. Experimental procedure and methods

2.1. Materials

Toluene-2,4-di-isocyanate (TDI ≥ 95%), Congo red (CR, C.I. 22120) eriochrome black, (EB, C.I. 14640), bromocresol purple sodium salt (BP, ≥ 90%), toluidine blue (TB, C.I.52040), crystal violet (CV ≥ 96%), brilliant green (BG ≥ 98%), methylene blue (MB ≥ 97%), β-cyclodextrin (CD ≥ 97%), cellulose microcrystalline (CC - for thin-layer chromatography, USP), and pyridine (anhydrous ≥ 99.8) were purchased from Merck. Dimethylformamide (anhydrous DMF ≥ 99.8), sodium hydroxide (NaOH ≥ 99% and 0.1 N solution), hydrochloride acid (0.1 N HCl), and 30% aqueous solution of hydrogen peroxide were supplied by Chempur. Methanol (CH_3OH ≥ 99.8%), sodium and calcium chlorides (NaCl ≥ 99%and $CaCl_2$ ≥ 99%) as well commercial humic acids containing 50% of humic acids and 50% fulvic acids (HA, 90% dry matter)

were purchased from Chempur and Agraplant, respectively. Potassium bromide (KBr spectroscopy grade) was delivered by Fisher Scientific and dried before use. Coffee grounds 100% Arabica were obtained from a local cafe as waste obtained from an espresso machine. All chemicals were used without further purification. Water purified by a Hydrolab-system was used to prepare the stock solutions (HLP-SPRING, temp. 22 °C, κ = 2.70 μS). The treated effluents were obtained from the Gdansk East sewage treatment plant. The final form of each adsorbent was obtained after drying material in a moisture analyzer (MA50/1. R, Radwag) and grinding in a ball mill (Pulverisette 7 classic line, Fritsch).

2.2. Instrumental analyzes

Fourier transform infrared (FT-IR) spectra were performed on a Thermo Nicolet iS10 using the KBr pellet method. The spectral resolution was 4 cm^{-1} and the scanning range was from 400 to 4000 cm^{-1}. The specific surface area was measured by the Brunauer–Emmett–Teller (BET) method (Brunauer et al., 1938), and pore size distribution (PSD) was measured using the classical Barrett–Joyner–Halenda (BJH) model (Barrett et al., 1951). The simultaneous TG–DTA curves were obtained with a heating rate of 10 °C min^{-1} in temperature range of 30–700 °C. The experiments were carried out under nitrogen atmosphere at a flow rate of 50 mL min^{-1}, in a SETSYS - 1200 (TG-DTA 1600 °C) system. The surface morphology of adsorbents was studied using scanning electron microscopy (SEM) on a Quanta FEG 250 scanning electron microscope operating at 10 kV. The surface charge properties of the adsorbents were investigated by Zeta potential measurements conducted at a different equilibrium pH using a Nano-ZS Zetasizer (Malvern Instruments Inc.). The elemental FLASH 2000 analyzer operating in the dynamic separation technique was used to measure the content of carbon, hydrogen, and nitrogen. The oxygen content analysis was performed by the device in the pyrolysis mode. The determination of surface functional groups was based on the Boehm titration method (Boehm, 1966). The degree of substitution (DS) was estimated with respect to the monomeric unit (anhydroglucose) using elemental analysis (Qin et al., 2017; Zhang et al., 2021), FTIR spectroscopy (Li et al., 2019) and additionally for systems containing β-CD phenolphthalein complexation (Cadena et al., 2009; Goel and Nene, 1995; Mohamed et al., 2012). PZC was evaluated according to titration procedures described in the literature (Abu-Danso et al., 2019; Kyzas, 2012; Leone et al., 2018; Luo et al., 2019; Oliveira et al., 2008). The water holding capacity (WHC) was determined in a manner typical for this type of material (Ballesteros et al., 2014).

2.3. Preparation and characterization of adsorbents

2.3.1. Coffee grounds (CG) preparation

Air-dried Arabica coffee grounds (100 g) were extracted three times with distilled water (3 × 0.5 L) at boiling point for 30 mins each time. The grounds were then filtered off under reduced pressure and dried at 120 °C for 4 h in the dryer and then they were kept for 4 h in the moisture dryer. The obtained dark powder (80 g) was stored in tightly closed containers.

2.3.2. Preparation of cellulose from coffee grounds (CGC)

CG (30 g) was quantitatively transferred to a flask containing 1% (w / v) H_2O_2 solution (1.5 L). The suspension was adjusted to pH 11.5 with NaOH and allowed to stir gently at room temperature (25 °C) for the indicated length of time (48 h). Subsequently, pH corrections were made during the reaction in the first hour. The insoluble residue was collected by filtration, washed with distilled water until the pH of the filtrate was neutral, and then dried at 120 °C for 4 h in a laboratory dryer and another 4 h in a moisture analyzer. The yield obtained was dark yellow, and weighed 14 g.

Table 1
Models of adsorption isotherms and applied plots in the research.

Model *		Ref.
Langmuir	$q_e = \frac{q_{max} K_L C_e}{1 + K_L C_e}$	(Langmuir, 1917)
Freundlich	$q_e = K_F C_e^{\frac{1}{n}}$	(Freundlich, 1906)
Sips	$q_e = \frac{q_{max} K_s C_e^{\frac{1}{n}}}{1 + K_s C_e^{\frac{1}{n}}}$	(Sips, 1948)

*q_{max}—maximum adsorption capacity (mg g−1); K_L—adsorption equilibrium constant (L mg−1); R_L—the separation factor; K_F—adsorption capacity constant (mg1−1/n L1/n g−1); K_s—Sips equilibrium constant [(mg L−1) − 1/n], n—heterogeneity factor.

2.3.3. Synthesis of modified cellulose (CT), cellulose-β-cyclodextrin material (CTCD), and β-cyclodextrin material (CD-1)

Polymers were prepared according to the described procedure (Huang et al., 2012) with a few modifications. CC (10 g) or CD (10 g) or their mixture 1: 1 (5 g CD and 5 g CC) were suspended in dry pyridine (100 mL) at 80 °C. Then, TDI (9.7 g) was added dropwise over an hour. After being magnetically stirred at 80 °C for 3 h, the mixtures were cooled to room temperature and 300 mL of acetone was poured. The precipitates were filtered off and after drying were purified in Soxhlet apparatuses with ethanol for 8 h. The obtained materials were dried in an oven at 120 °C, ground, and dried again in a balance drier at 120 °C.

2.3.4. Synthesis of β-cyclodextrin material (CD-2) synthesis

CD-2 polymer was synthesized according to the reported method with one modification by changing the molar ratio of TDI:CD from 10:6:1. (Anne et al., 2018).

2.4. Adsorption experiments

2.4.1. Analytical method of pollutant concentration determination

The concentrations of CV were measured spectrophotometrically, (UV-Vis, model Hach Lange dr 6000). The effect of pH and aquatic environment on calibration curves and λ_{max} = 591nm were studied. Each of the determinations was repeated at least three times. The reliability of the results was considered on the basis of the analysis of variance (Anova test). Dye removal efficiency (RME) was determined by the Eq. (1),

$$RME(\%) = \frac{C_0 - C_t}{C_0} \times 100 \quad (1)$$

where the RME (%) was the efficiency of CV removal, C_0 (mg L^{-1}) and C_t (mg L^{-1}) were initial concentration and concentration at time t of dye in the sample.

2.4.2. Adsorption isotherms

1 mg of the adsorbent was added into the 5 mL of CV solution (with initial concentration ranging from 2.45 to 407.98 mg L^{-1}) and shaken on digital vortex mixer at 700 rpm at 25 °C for 20 min. Then the supernatant liquid was sampled and filtered. The adsorption equilibrium concentration of each was measured. Three isotherm equations were used in the analysis of experimental data, Langmuir, Freundlich, and Sips (Table 1).

2.4.3. Thermodynamic analysis

The key thermodynamic parameters of adsorption were determined on the basis of the below Eq. (2)–(4).

$$\ln\left(K_e^0\right) = \frac{-\Delta H^0}{RT} + \frac{\Delta S^0}{R}, \quad (2)$$

Table 2
Description of the kinetic models used in the calculations.

Kinetic model		Ref.
Pseudo-first order	$q_t = q_e e^{(-k_1 t)}$	(Bello et al., 2021)
Pseudo-second order	$\frac{t}{q_t} = \frac{1}{K_2 q_e^2} + \frac{t}{q_e}$	(Wang et al., 2021)
Avrami fractional-order model	$q_t = q_e(1 - e^{-(k_{AVt})^n}$	(Sivarajasekar et al., 2018)
Elovic	$q_t = \frac{1}{\beta}\ln(\alpha\beta) + \frac{1}{\beta}\ln(t)$	(Martín et al., 2019)

$$\Delta G^0 = -RTln(K_e^0), \quad (3)$$

$$K_e^0 = \frac{KM_a C_a^0}{\gamma}, \quad (4)$$

where ΔS^0, ΔH^0, ΔG^0 standard enthalpy, entropy and free energy and K_e^0 is a dimensionless thermodynamic equilibrium constant, which is calculated from the best isotherm fitted K (L g^{-1}), M_a, and C_a^0 are molecular weight and standard concentration of the adsorbate (1 M), and γ is the coefficient of activity, respectively (Lima et al., 2019).

2.5. Adsorption kinetics in batch experiments

100 mg of adsorbent was added to three plastic vials containing 50 mL of CV solution (10.20 mg L^{-1}). The vials were shaken on digital vortex mixer at 700 rpm at 25 °C. The supernatant liquids were sampled at different times (0, 1, 3, 6, 10, 15, 20, 30, 45, and 60 min) and filtered using Whatman Grade 540 filter paper. The amount of CV bound to the adsorbent was determined by Eq. (5).

$$q_t = \frac{(C_0 - C_t)V}{m} \quad (5)$$

where the m (mg) is the adsorbent dosage and the V (mL) is the solution volume used in the study. In further calculations, four kinetic models were used to determine kinetic constants using graphical methods (Table 2).

2.6. Effects of the dosage of the adsorbent, pH humic acid, and salts

The effect of adsorbent dosage was studied by the addition of the adsorbent (1–100 mg) to the plastic vials (5 mL) containing CV solution (10.20 mg L^{-1}) and shaken on a digital vortex mixer at 700 rpm at 25 °C for 20 min. Then the supernatant liquid was sampled and filtered. The adsorption equilibrium concentration of each was determined colorimetrically. The influence of ionic strength was investigated analogously, using drug solutions enriched with appropriate salts, humic and fulvic acids, and the pH was adjusted to the appropriate value in the range from 2 to 11 with 0.1 N HCl and 0.1 N NaOH.

2.7. Real wastewater treatment

The wastewater was used to make solutions of dyes (Table S11). Relatively high concentrations of dyes, compared to those determined in the natural environment, were used intentionally as a simulation of an industrial sewage system. The adsorption procedure was the same as for model water samples with one difference; the wastewater was used to prepare the solutions instead of pure water. The 5 mL of dye (0.025 mmol L^{-1}) solutions were added to plastic vials containing 10 mg of adsorbent, individually. The vials were sealed and the mixtures were shaken on digital vortex mixer at 700 rpm for 20 min at 25 °C. Then the supernatant liquid was sampled and filtered. The adsorption equilibrium concentration of each was measured.

2.8. Regeneration

100 mg of material was added to the vial containing 50 mL of the CV solution (10.20 mg L^{-1}). The mixture was shaken in a digital vortex mixer at 700 rpm (25 °C, 20 min). After five minutes, the solution was decanted from the surface of the precipitate and in its place, 20 mL of methanol was added, soaking for 10 min. The procedure was repeated until no CV was found in the filtrate, and finally, the precipitates were washed with distilled water (20 mL). The adsorption-desorption experiment was performed five times. Scheme 1.

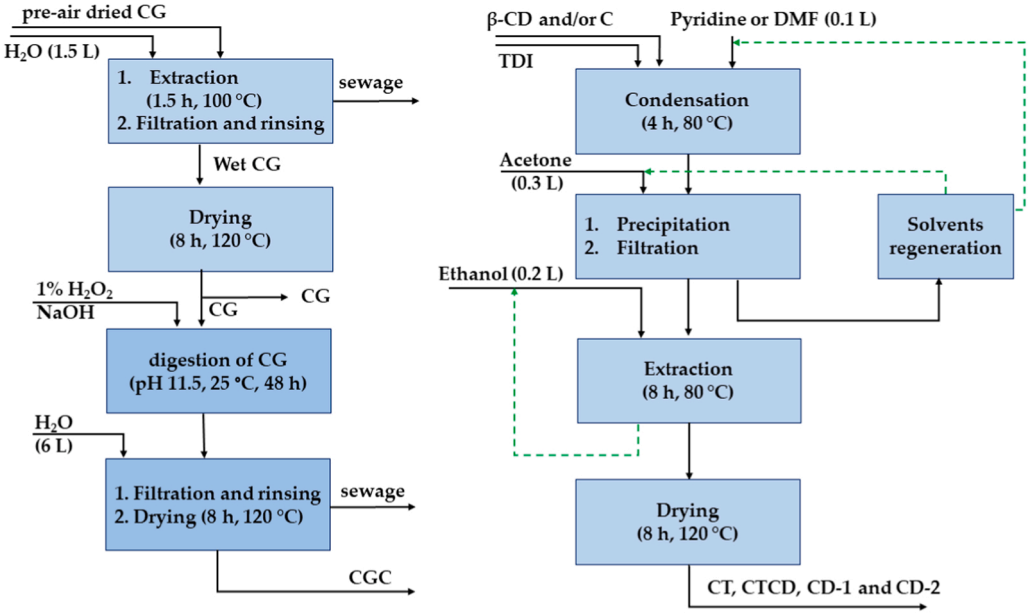

Scheme 1. Simplified schematic diagrams showing the preparation of CG, CGC, CT, CTCD CD-1, and CD-2 adsorbents.

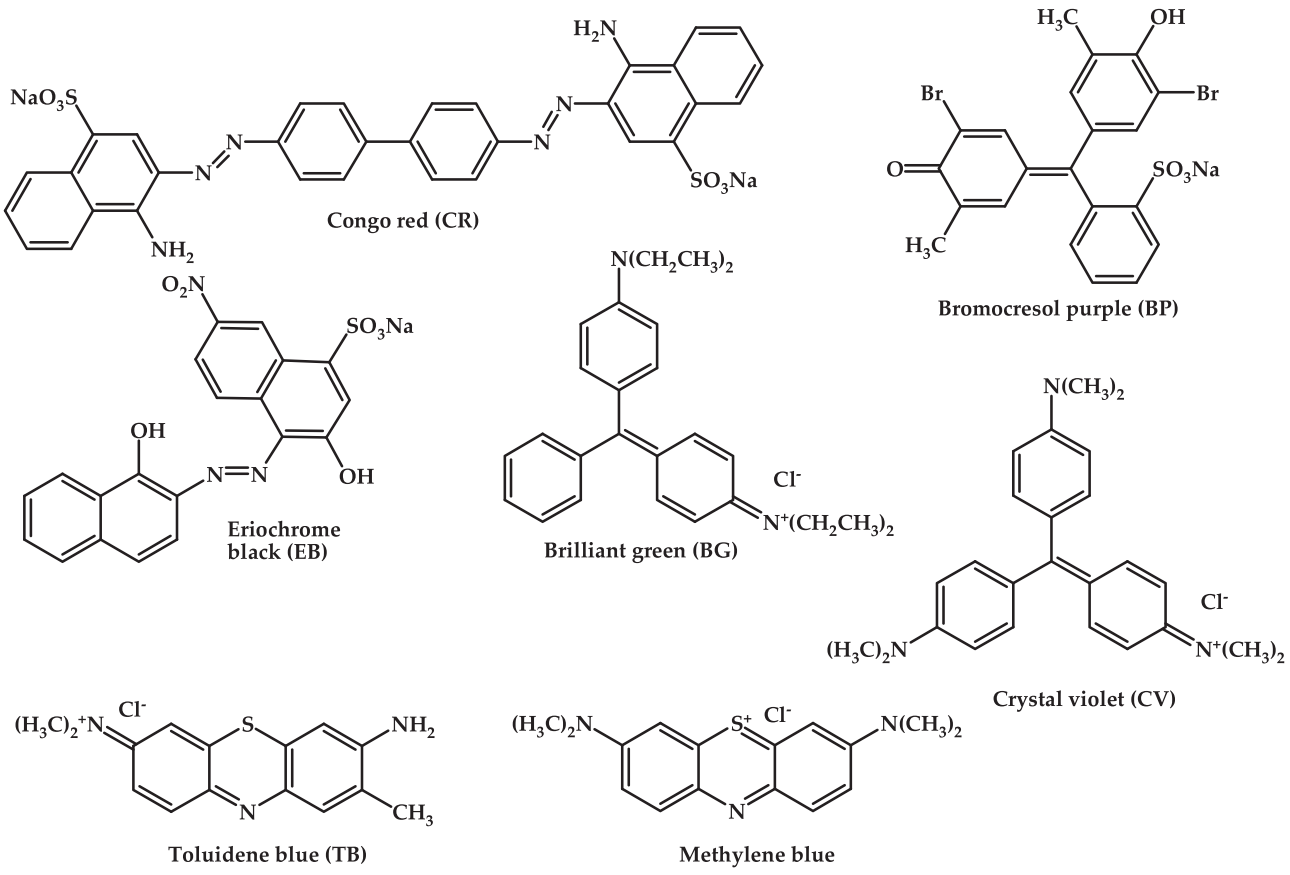

Fig. 1. Chemical formulas of studied pollutants.

3. Results and discussion

3.1. Material design and characterization

The study attempts to take a holistic approach to the production of organic sorbents with potential use in the treatment of wastewater containing dyes. First of all, attention was paid to reducing the number of unit operations, and thus the resulting waste. Nutritional waste such as CG has already been used for dyes adsorption in raw and pretreated forms (Ahalya et al., 2014; Ayalew and Aragaw, 2020; Kyzas, 2012; Oliveira et al., 2008), with different results. In this work, CG was subjected to extraction with boiling water to diminish its amount. As a consequence, the content of water-soluble components was reduced, obtaining a material that was more durable in subsequent cycles. Therefore, the processing of organic waste into new adsorbents is only justified in the case of obtaining a significantly higher degree of contamination removal from aqueous solutions. The CG was transformed into a material enriched with cellulose fibers (CGC) by a bleaching process. The bleaching processes generate large amounts of wastewater, characterized by high values of total organic carbon (TOC) and inorganic compounds (Börjesson and Ahlgren, 2015; Brännvall, 2009; Mohit et al., 2014). Microcrystalline cellulose (CC) was used in the research in its basic form and modified in the condensation reaction with TDI. This modification was aimed at reducing hydrophilicity and obtaining additional π-π interactions with aromatic dyes.

It was time effective to synthesize materials containing CD, which is known for the formation of supramolecular complexes with aromatic compounds. The incorporation of CD molecules usually increases the sorption capacity of the system. Thus, the cross-linked systems resulting from the reaction of TDI with cellulose and (or) CD were also synthesized.

In summary, seven adsorbents were obtained, based on D-glucose oligomers and polymers, modified to a different extent. The mild CG bleaching conditions were designed to remove free phenolic groups while retaining others (Table S1). The goal was achieved, the content of phenolic groups was reduced by almost 60% while not significantly lowering the content of carboxyl and basic groups. The obtained material differed significantly from commercial microcrystalline cellulose. All raw materials used in the research contain free primary and secondary hydroxyl groups. By using an appropriate solvent, the selectivity of the substitution of these groups can be influenced. A simple system to investigate this phenomenon is CD, which has been modified in pyridine, which supports the selective substitution of primary hydroxyl groups, and in DMF, which does not. Such subtle changes lead to materials with varying degrees of cross-linking and properties.

FTIR spectroscopy is an inexpensive and widely available technique that enables the analysis of sparingly soluble organic compounds in water and organic solvents. Via FTIR, basic functional groups and hydrogen bonds can be identified. The proportion of crystalline and amorphous forms and the water content can be determined and was important for adsorption. Fig. 1 shows the spectra recorded during the FTIR analysis of the discussed materials in two forms: before after five uses. The comparisons show that the materials do not change after five adsorption-regeneration cycles. At first glance, the FTIR CD and CC spectra appear very similar. However, when analyzing more closely, differences are noticed, which are the result of the different spatial arrangement of monomer (glucose) molecules in the cyclic oligomer and the linear polymer and are within the wavenumber range 1630–1440 cm^{-1} (Figs. 2a and 2b).

The peaks at 1636.38 cm^{-1} (CD) and 1637.27 cm^{-1} (CC) were responsible for the vibrations of adsorbed water molecules; 1412.06 cm^{-1} (CD) and 1431.49 cm^{-1} (CC) were related to the degree of crystallinity while 896.43 cm^{-1} (CC) to the degree of amorphousness (Åkerholm et al., 2004). Comparing the CG and CGC spectra, it was seen

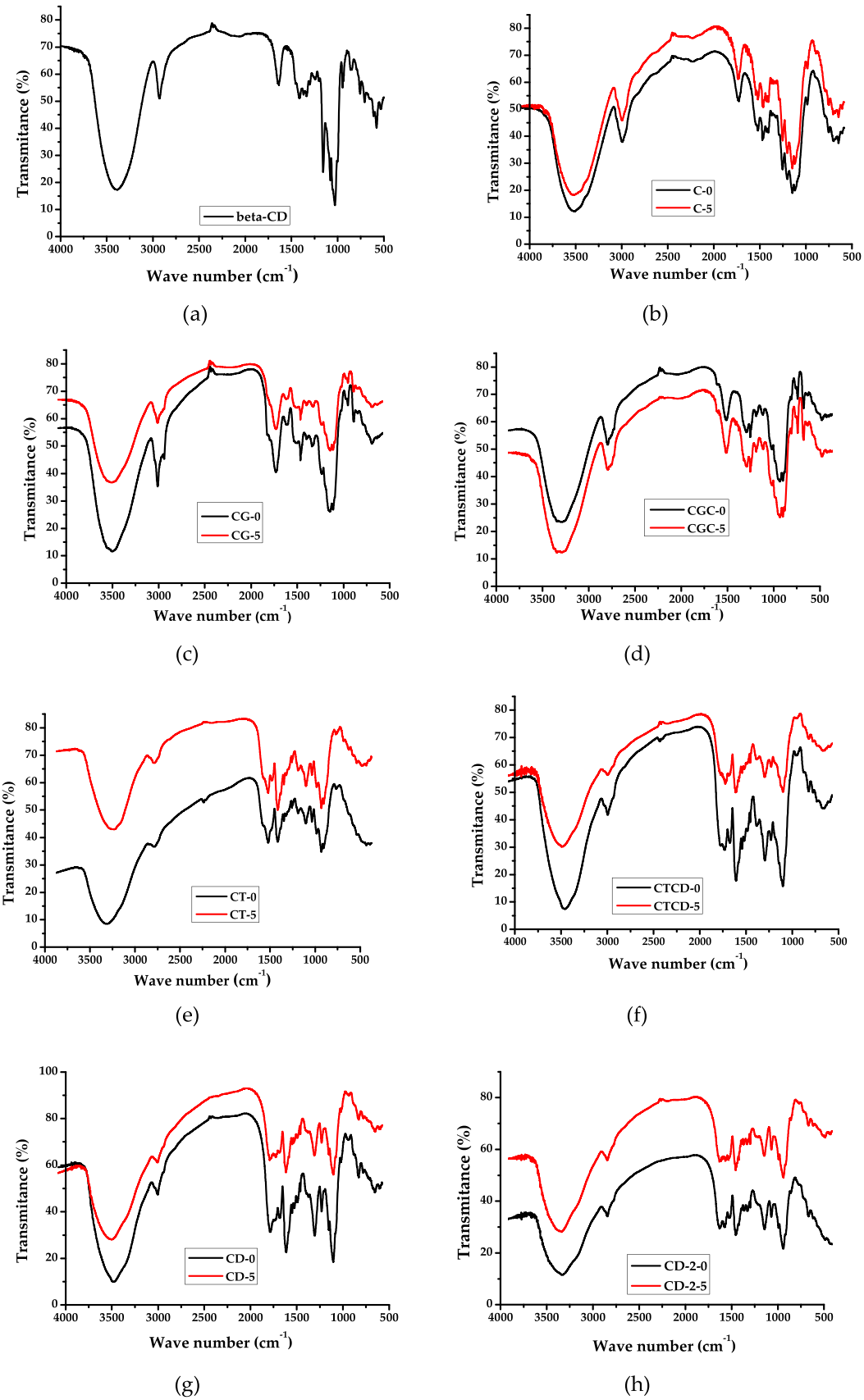

Fig. 2. Recorded FTIR spectra of sorbents in KBr. The adsorbents not used are marked in black, and the adsorbents after the fifth regeneration cycle are marked in red.

that CG contained more adsorption water, and the carboxyl groups, the presence of which was confirmed in Boehm's method, were probably in the deprotonated form (1542.59 cm^{-1}) (Figs. 2c and 2d). A higher proportion of the crystal structure guarantees a higher degree of order and better mechanical properties. The intensity of the bands described with wave numbers proximate the range of 1420 – 1430 cm^{-1} and 898 cm^{-1} corresponds to the content of the crystalline and amorphous structure in cellulose, as was mentioned (Åkerholm et al., 2004). The ratio between the two bands determines the empirical index of crystallinity proposed by Nelson and O'Connor (Nelson and O'Connor, 1964) as the lateral order index, which is correlated to the overall degree of order in the cellulose (LOI). The ratio of the bands at 1372 and 2900 cm^{-1} is the total crystal indicator of cellulose (TCI) (Nelson and O'Connor, 1964). The intensity of hydrogen bonding (HBI) of cellulose is closely related to the crystal system as well as the amount of bound water and can be determined from the ratio of absorbance bands at 3400 and 1320 cm^{-1} (Oh et al., 2005). The comparisons in Table S2 clearly showed that CC had the most ordered structure. The bleaching process slightly improved the order of particles in the material, while the attachment of β-CD cyclic spatial systems to the CC fiber gave the opposite effect. Modification of CC with isocyanate significantly increased the value of the total crystal indicator of cellulose, thus radically reducing the intensity of hydrogen bonds formed. The amount and strength of hydrogen bonds significantly affected the sorption capacity of the material, containing cellulose fibers, so they should be carefully examined. CTCD showed the lowest hydrogen bond energy at 3567 cm^{-1}, probably due to the amount of weakly bound water, enclosed in CD tori. On the other hand, CT and CG showed higher values of hydrogen bond energies at the same wavenumber, which may be the result of the formation of multiple intramolecular hydrogen bonds between adjacent urethane (CT) and phenolic groups in lignin (CG). Hydrogen bond energies for the bands 3423 cm^{-1} and 3342 cm^{-1} are highest for CG and CT. The energy values at 3278 cm^{-1} and 3221 cm^{-1} in relation to allomorphic forms of cellulose indicate a much greater proportion of intermolecular hydrogen bonds occurring in triclinic I_α cellulose (3221) than in monoclinic cellulose I_β (Table S3).

The FTIR spectra of the adsorbents obtained in the C and CD condensation reactions with TDI and it did not contain the 2275–2250 cm^{-1} bands, which proves the transformation of isocyanate groups into urethane groups (about 1715 cm^{-1}). All urethane derivatives were further characterized by determining the degree of substitution. The various techniques used gave quite convergent results, showing a single substitution of the monomeric unit (anhydroglucose) indicating a high degree of cross-linking (Table S4).

It is customary for adsorbents to determine BET isotherms to determine the specific surface area. Measurements were carried out at low temperature using nitrogen. The BET theory assumes that the adsorption energy was independent of the gas molecules' adsorption sites, which interact only in the vertical direction, while the side effects between adjacent adsorbed molecules were negligible (Brunauer et al., 1938). The BET isotherms obtained for CGC, CT, CTCD, and CD-1 belonged to type III (Fig. S1). The determined CC coefficients were less than one, and in the case of CGC and CTCD, they were even negative. These results specify the formation of a multilayer, with no asymptote on the curve. CG, C, and CD-2 give type IV isotherms suitable for partial capillary condensation of nitrogen at a pressure less than the saturation pressure of the gas (Fig. S1). In areas of lower pressure, a monolayer was formed, followed by a multilayer system. This is typical of BET surfaces of mesoporous materials including CG, C, and CD-2. When plotting the BET equation, the plot should be linear with a positive slope. If such a grapHis not obtained, the BET method is insufficient to determine the surface area of the material. Therefore, the determination of the CTCD BET surface area was not possible and in this case of CT and CD-2 were not entirely reliable (Table S5.) The next method developed by Barrett, Joyner, and Halenda, BJH assessments the pore size distribution (PSD) on the basis of the isothermal physisorption equilibrium state. The BJH

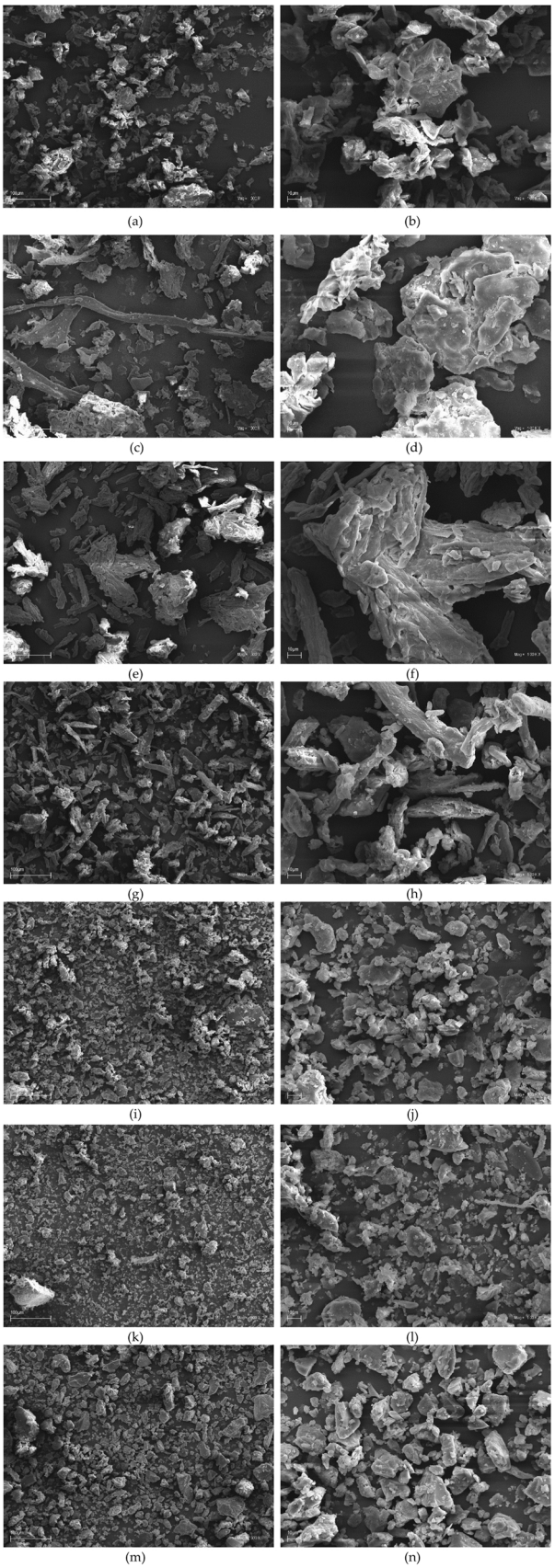

Fig. 3. SEM images of the obtained materials, recorded at mag. 300x and mag. 1000x: CG (a, b); CGC (c,df); CC (e, f); CT (g, h); CTCD (i, j); CD-1 (k, l); CD-2 (m, n).

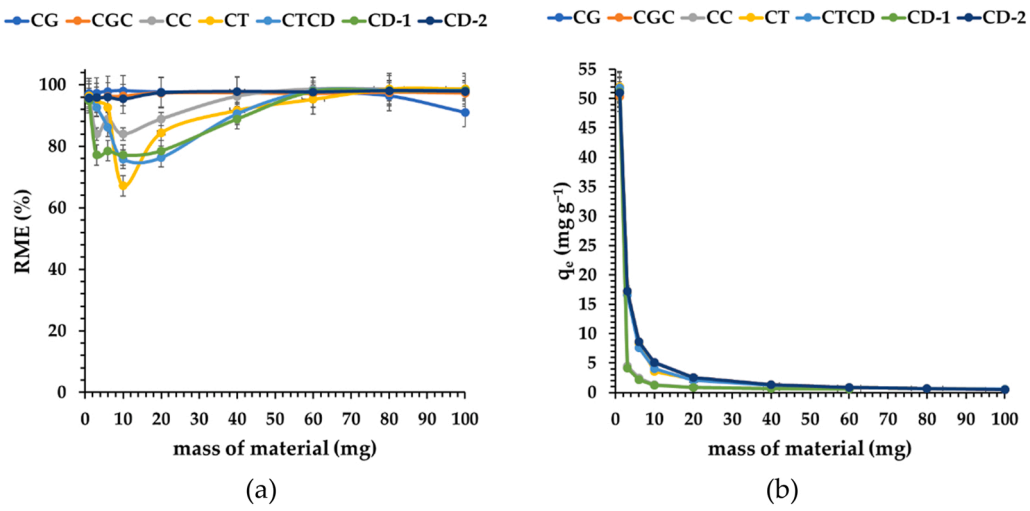

Fig. 4. Effect of the adsorbent mass on the removal efficiency (a) and adsorption capacity (b); $t_{contact}$= 20 min, C_{CV} = 10.20mgL^{-1}, V_{CV} = 5*mL* and $m_{CVsorbent}$ = 1 – 100mg.

theory implements follow basic rule book; first, the shape of the pores was cylindrical, and second, the amount adsorbed was due to both physical adsorption on the walls of the pores and capillary condensation at mesopores (Barrett et al., 1951). All adsorbents were mesoporous. In the case of CGC, macropores also have a large share (Table S5). All materials retain water in their structure and swell (Table S6). The CGC changed the most, fibers became larger which was accompanied by a more than threefold increase in material volume. This phenomenon was often observed with cellulose-containing materials and not only (Ballesteros et al., 2014; Ferro et al., 2014; Hoti et al., 2021; Pagalan et al., 2020; Zheng et al., 2018).

Each adsorbent viewed under an electron microscope was a cluster of particles differing in size and structure, despite the use of the same grinding and screening method. CG CGC contained the longest monofilaments of cellulose 154.55 μm (Figs. 3a) and 472.73 μm (Fig. 3c), and particles with a very diverse structure and size of 3.16–60.02 μm and 7.27–247.27, respectively. Microcrystalline cellulose was a mixture of particles ranging in size from 10.91 μm to 190.91 μm. (Figs. 4e and 4f). CT was a cluster of particles with an oval shape and size of 76.36 × 56.36 μm and oblong about dimensions 163.36 × 21.82 μm. (Fig. 3g), and those containing CD were the most fragmented (Fig. 3i-n). CTCD mainly contained relatively small particles 2.73 μm and a few bigger ones (101.82 μm). The smallest particles with a length of 1.82 form CD-1 and CD-2, with the difference that the second one contained the greater proportion of particles with a length of 94.55 μm.

The materials differ essentially in the pHvalues at which the zero charge points were determined and arranged in the series CD-1 > CD-2 > CT> CGC> CC> CTCD> CG. The differences were quite large between the extreme materials and amount to three units (Fig. S2 and Table S7). The large size and tendency to swell did not allow to determine the zeta potential of the most fibrous materials (CG and CGC). CD-1, despite its small dimensions, did not form sufficiently stable suspensions in aqueous solutions, which also made it impossible to perform the measurement. For the remaining materials, isoelectric points were determined and the distribution of charges was specified. Each of the adsorbents had two isoelectric points, which define the ranges of the charge distribution. Interestingly, the CTCD surface charge in almost the entire range of the tested pH2–11 is negative (Fig. S3).

All materials were thermally stable. At temperatures up to 150 °C, they lose water (Table S8). The share of unstably bound water was the largest, which is removed below 100 °C. The proper decomposition began above 250 °C and mainly had the nature of endothelial transformation, only in the case of sorbents containing β-cyclodextrin, exothermic peaks were recorded. Figures exhibited the TG and DTA curves and a detailed description was included in the supplementary materials (Fig. S4 and Table S9). An attempt was also made to determine the hydrophobic properties of the obtained materials. In the two-phase tests carried out, consisting of toluene and distilled water, only microcrystalline cellulose immediately found itself in the inorganic phase, in which it also remained after mixing. The remaining materials initially stopped at the interface. After intensive mixing, they fell into the water phase. The exception was CT, which was completely dispersed in the organic phase. Based on the estimated hydrophobicity index, the materials can be arranged in the following series: CT> CTCD> CG> CGC> CD-1 > CD-2 > CC (Table S10).

3.2. Adsorption studies

3.2.1. Effect of the adsorbent mass

CV adsorption is one of the fastest processes. Using the constant concentration of the adsorbate and the variable adsorbent, the maximum degree of dye removal from the solutions were obtained for the value of 1 mg. This was due to the largest excess of dye in relation to the weight of the adsorbent used. The RME value for CGC and CD-2 in the entire range of tested masses is practically constant. In the case of CG, it also initially decreased after exceeding the value of 80 mg. In other cases, the dependence of RME on the mass of the material follows a different course. The maximum value was achieved for the smallest weights and the lowest for 10 mg of materials, followed by an increase in the RME value to the original cutoff value. The adsorbate excess for 1 mg of the adsorbent is tenfold, for 10 mg it is 1.05, and in the extreme case 0.105. Reducing the concentration increases the number of degrees of freedom in filling the surface without the need to penetrate deeper structures of the materials, as a result, the surface of the materials is only partially used (Fig. 4). The study indicated that the most reasonable adsorbent concentration during the determination of isotherms would be the value of 0.2 g L^{-1}. For this concentration, very similar values of the RME parameter and q_e were obtained for all materials. The use of uniform conditions in our opinion allows a better comparison of materials. The literature describes adsorption processes in which the authors used very low sorbent concentrations with success (Badruddoza et al., 2017; Bhadra et al., 2017; Ching et al., 2020; Liu et al., 2020; J. wei Wang et al., 2021; Younis et al., 2020). In the case of cyclodextrin materials, it is even desirable to be able to use every element of the structure and not just the interiors of the torus. During the first stage of sorption, supramolecular complexes are formed (Hemine et al., 2020). If the adsorbate concentration is high enough, subsequent molecules locate outside the torus (Huang et al., 2020). In the case of removal of

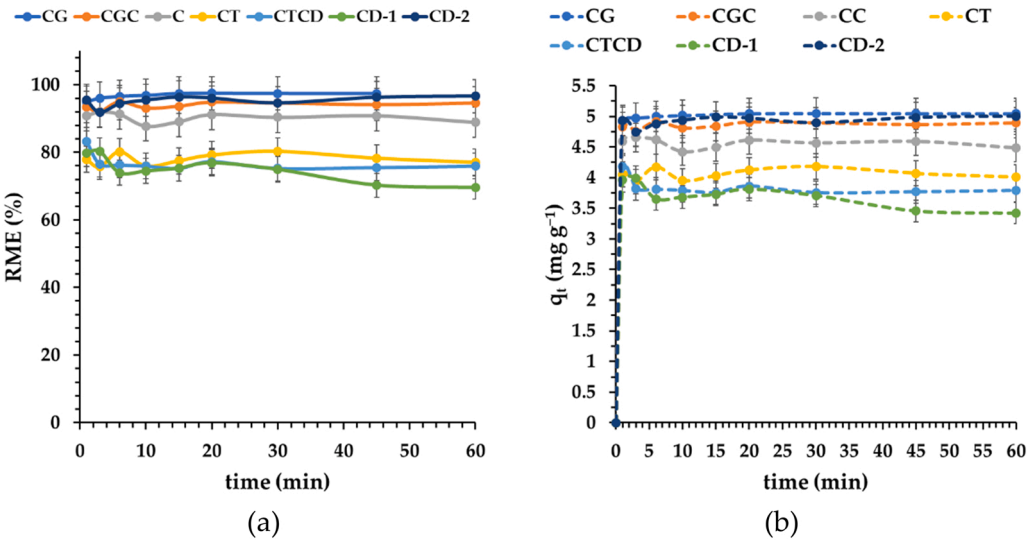

Fig. 5. Effect of the time on the removal efficiency ($t_{contact}$=60 min),(a) adsorption capacity (b);C_{CV} = 10.20mgL^{-1}, and $m_{CVsorbent}$ = 10mg.

Table 3
Kinetic model constants of single−component mixtures and their error analysis.

Parameters	CG	CGC	CC	CT	CTCD	CD-1	CD-2
Pseudo −first order							
q_e (mg g^{-1})	5.02	4.86	4.56	4.06	3.84	3.71	4.93
k_1 (g min^{-1} mg^{-1})	3.79	5.05	221.76	249.40	263.91	272.92	205.04
R	0.9998	0.9995	0.9987	0,9978	0.9942	0.9870	0.9988
R^2	0.9997	0.9980	0.9975	0.9956	0.9885	0,9742	0.9976
R_{adj}	0.9996	0.9980	0.9968	0.9943	0.9853	0.9669	0.9969
X^2	0.0016	3.881	0.01	0.0153	0.0380	0.0837	0.0101
Pseudo −second order							
q_e (mg g^{-1})	5.04	4.86	4.56	4.06	3.84	3.72	4.93
k_2 (g min^{-1} mg^{-1})	6.74	38.78	55.02	55.02	90.67	96.14	38.60
R	0.9999	0.9994	0.9987	0.9987	0.9940	0.9867	0.9989
R^2	0.9999	0.9990	0.9974	0.9974	0.9879	0.9736	0.9978
R_{adj}	0.9999	0.9987	0.9966	0.9966	0.9844	0.9661	0.9970
X^2	0.0154	0.0052	0.0116	0.0116	0.0466	0.0918	0.0104
Avrani							
q_e (mg g^{-1})	5.02	4.86	4.56	4.06	3.84	3.71	–
k_{AV} (g min^{-1} mg^{-1})	0.262	2.70	3.29	4.32	17.93	1.68	–
n	14.47	1.87	67.33	57.78	14.72	162.58	–
R	0.9999	0.9995	0.9987	0.9977	0.9943	0.9870	–
R^2	0.997	0.9985	0.9975	0.9956	0.9885	0.9742	–
R_{adj}	0.9996	0.9977	0.9962	0.9934	0.9828	0.9614	–
X^2	0.0016	3.88	0.0098	0.0154	0.0380	0.0837	–
Elovich							
β (g mg^{-1})	13,433.32	16,789.27	18,607.0	14,948.86	21,237.29	26,062.84	1624.08
α (g mg^{-1} min^{-1})	2.60	2.74	2.97	3.30	3.62	3.82	2.70
R	0.9527	0.9509	0.9387	0.9481	0.9148	0.8909	0.9528
R^2	0.9068	0.9037	0.8808	0.8983	0.8366	0.7935	0.9073
R_{adj}	0.8757	0.8762	0.8467	0.8693	0.7899	0.7935	0.8808
X^2	0.9617	0.303	0.8998	0.6980	0.9598	1.0947	0.8247

micropollutants, only a minimal amount of adsorbent ensures its full utilization (Hu et al., 2020; Erdös et al., 2020; Yang et al., 2019).

3.2.2. *Effect of the contact time and adsorption kinetics*

To determine the appropriate contact time between sorption material and dye, a set of experiments were carried out (Figs. 5a and 5b). It was observed that in a minute equilibrium for CTCD is achieved; two more minutes were needed for CC and CD-1. CT and CGC take twice as long. The steady-state was most slowly reached by CD-2 (15 min) and CG (20 min). The amount of dye adsorbed at equilibrium time was the lowest for CD-1 and the highest for CG and amounts to 3.99 mg g^{-1} and 5.04 mg g^{-1}, respectively. To investigate the mechanism controlling the adsorption process: pseudo-first, pseudo-second, and Avrami fractional order kinetic models were studied for the experimental data (Fig. S5). In the kinetic tests, 10 mg of the adsorbent was used per sample. The obtained parameters for the models are shown in Table 3. In the case of the tests performed for CC, CT, CTCD, CD-1, and CD-2, it seems that the dominant model was in the form of pseudo-first order kinetics. This might suggest that the mechanism of inclusion complex formation by inserting one ring inside the CD was a rate-controlling process in this system. The estimated CV adsorption rate constant is high and amounts to over 200 (g min^{-1} mg^{-1}) (Table 3). The pseudo-second order model provides a better description of the interaction between CG (CGC) and the dye. A fairly good fit to the Avrami model indicated that a phase transition may take place in the adsorption process. It is possible that the dye released from the salt is finally incorporated into the sorbent structure, which, due to its limited solubility, precipitates and is deposited on the material. Another explanation could be the reaction of

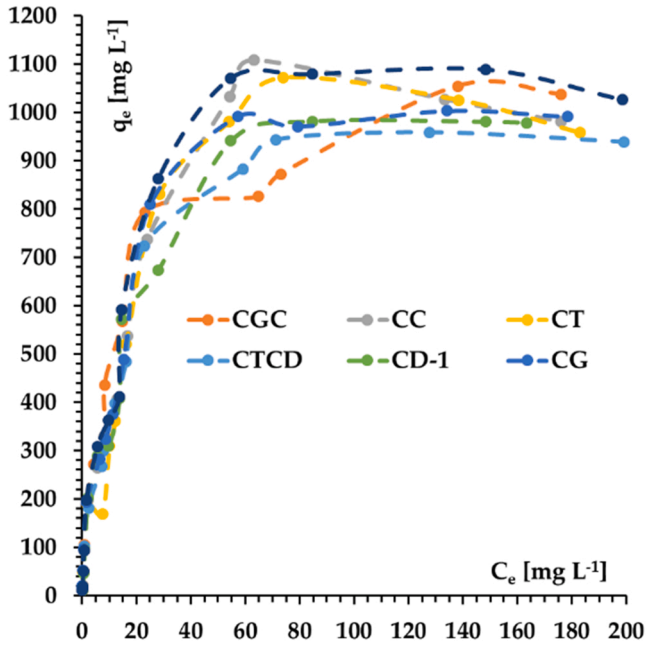

Fig. 6. Equilibrium adsorption isotherms of CV; $t_{contact}$= 20 min, C_{CV} = 2.45 – 407.98mgL^{-1}, V_{CV} = 5 mL and $m_{CVsorbent}$ = 1mg.

methine carbon which is a C-acid and can coordinate groups of a nucleophilic nature. Perhaps a necessary condition for this type of phenomenon is the presence of unsubstituted secondary hydroxyl groups. It can be proved by the lack of fit of this model for CD-2, which was the only one obtained in a non-selective manner. The adsorbate was chemisorbed onto a solid surface without desorbing the products and the rate of adsorption decreased over time due to increased surface coverage. The model which described this type of chemisorption was the Elovich equation in which α is the initial rate; the parameter β is related to the range of surface coverage and the activation energy for chemisorption. In this case, a worse fit of the model was obtained. Nevertheless, the parameter values can lead to chemisorption.

3.2.3. *Adsorption equilibrium*

For each sorbent, a better fit of the experimental data (Fig. 6. and Fig. S6) of the Langmuir then the Freundlich models were obtained (Table 4.) in terms of the R^2 coefficient. These results suggested that adsorption mainly proceeds with monolayer formation over a relatively uniform surface. The Langmuir model assumed that adsorption occurred at specific and localized sites and that all adsorption sites were energetically identical (Langmuir, 1916). Homogeneous sites were found by analyzing the SEM images (Fig. 3).

The Freundlich isotherm was used to describe multilayer adsorption and non-homogeneous surfaces with non-uniform heat distribution of adsorption. In the isotherm equation, the value of the n parameter, which determines the quality of the adsorption process, is extremely important (Lessa et al., 2018). The process is favorable when it is between 1 and 10. Among the tested adsorbents all meet this condition. The Sips model bridges the gap between the isotherms described so far and works well for localized adsorption without adsorbate-adsorbate interaction (Mohamed et al., 2012; Usman et al., 2021). As C_e approaches a low value, the Sips isotherm is efficiently reduced to Freundlich, while at high C_e it predicts the sorption properties of the

Table 4
The isotherm parameters for the adsorption of CV by studied sorbents.

Parameters	CG	CGC	CC	CT	CTC	CD-1	CD-2
Langmuir							
K_L (L mg^{-1})	0.056	0.074	0.055	0.0467	0.0567	0.055	0.056
q_{max} (mg g^{-1})	1168.14	1092.24	1220.40	1226.24	1100.37	1137.71	1235.32
R	0.9875	0.9906	0.9833	0.9772	0.9911	0.9908	0.9853
R^2	0.9743	0.9809	0.9667	0.9548	0.9821	0.9813	0.9706
Adj. R^2	0.9700	0.9777	0.9612	0.9473	0.9791	0.9782	0.9657
X^2	298.13	118.99	197.08	359.22	132.86	133.70	190.05
Freundlich							
K_F (mg$^{1-1/n}$ L$^{1/n}$ g^{-1})	181.22	181.22	187.51	168.68	170.02	164.35	199.204
n	2.78	2.79	2.77	2.66	2.79	2.66	2.87
R	0.9617	0.972	0.9487	0.9416	0.9599	0.9677	0.9508
R^2	0.919	0.9418	0.8930	0.8801	0.9144	0.9305	0.8966
Adj. R^2	0.9060	0.9321	0.8751	0.8601	0.9002	0.9189	0.8793
X^2	471.08	464.04	580.60	658.69	486.74	465.30	662.20
Sips							
K_S[(mg L^{-1})$^{-1/n}$]	0.0673	0.0612	0.0651	0.0645	0.0652	0.0551	0.067
n	1.36	0.86	1.344	1.17	1.22	1.001	1.29
q_{max} (mg g^{-1})	1073.07	1168.54	1123.99	1036.28	1034.34	1137.25	1157.18
R	0.9905	0.9910	0.9871	0.9920	0.9929	0.9908	0.9879
R^2	0.9768	0.9822	0.9711	0.9771	0.9838	0.9813	0.9731
Adj. R^2	0.9705	0.9773	0.9632	0.9709	0.9794	0.9762	0.9657
X^2	1566.29	91.528	978.97	24,794.63	412.58	134.23	675.83
Thermodynamic parameters							
ΔH^0 (kJ mol^{-1})	39.46	133.55	38.86	4.23	6.59	2.23	6.77
ΔS^0 (J K^{-1} mol^{-1})	227.3	505.75	221.92	119.17	126.56	56.56	127.08
ΔG^0_{293} (kJ mol^{-1})	-27.14	-14.63	-26.16	-30.69	-30.50	-31.52	-30.45
ΔG^0_{313} (kJ mol^{-1})	-31.70	-24.75	-30.60	-33.08	-33.02	-33.86	-33.00
ΔG^0_{333} (kJ mol^{-1})	-36.24	-34.86	-35.05	-35.46	-35.55	-36.13	-35.55
R^2	0.99677	0.99963	0.99642	0.99842	0.98453	0.99289	0.99788
RSS	0.01032	0.00742	0.01323	6.8958E-5	0.00168	8.78268E-5	2.36836E-4
Adj. R^2	0.98709	0.99932	0.98571	0.99369	0.9386	0.97167	0.99155
Intercept	27.34106	60.83148	26.69261	14.33415	15.22238	13.8634	15.28478
Slope	-4746.21068	-16063.54095	-4673.54845	-508.74196	-793.07671	-269.50657	-814.21906
Intercept SE	1.22734	0.95234	1.27208	0.09183	0.45079	0.10364	0.17019
Slope SE	382.58742	296.86606	396.53433	28.62621	141.14505	32.30614	53.05127

Table 5
Maximum adsorption capacity of natural and semi-natural adsorbents given in the literature for CVs and their regeneration methods.

Sorbent	Adsorption capacity (mg g^{-1}) at 25 °C	Desorption conditions	References
EDTA-Cross-Linked β-Cyclodextrin	0.11	Ethanoic solution of acids, precipitate, rising with water to pH= 7	(Zhao et al., 2015)
Lignin-Rich Adsorbent	10.05	2 M solution of NaOH; HCl addition to pH= 2, precipitate rising with water to pH= 7	(Menkiti and Aniagor, 2018)
nanosilica-supported poly β-cyclodextrin sorbent	34.50	1 M HCl, ethanol and water	(Chen et al., 2018)
β-cyclodextrin carbon-based nanoparticles with	87.87	No data	(Younis et al., 2020)
Avocado seed powder	95.9	No data	(Bazzo et al., 2016)
Coffee waste	125.00	No data	(Lafi et al., 2014)
supramolecular hydrogels in form of cyclodextrin pseudorotaxane and clay	199.00	No data	(Zhang et al., 2019)
grapefruit peel	254.16	1 M NaOH, precipitate rising with water to pH= 7	(Saeed et al., 2010)
CGC	1092.24	Methanol	This work
CG	1168.14	Methanol	This work
CD-2	1235.32	Methanol	This work
CC	1220.40	Methanol	This work
CT	1226.24	Methanol	This work
CTCD	1100.37	Methanol	This work
CD-1	1137.71	Methanol	This work
β-cyclodextrin modified electrospinning fibers	1049.88	Ethanol, pH= 4	(Jia et al., 2019)

Langmuir monolayer. The Sips isotherm equation was characterized by a dimensionless heterogeneity coefficient n, which was used to describe a system inhomogeneity if the value of n is between 0 and 1. When $n = 1$, the Sips equation became the Langmuir equation and represented the homogeneity of the adsorption process. All sorbents represent a good fit to the Sips model. The parameter n for six of the seven sorbents was greater than one which might indicate that sorption of one (first) CV molecule increased sorption of more others. These values of the obtained q_{max} were very high and in any case. These results indicated that the correct choice of materials was made. Nevertheless, from the point of view of the adsorption process itself, used coffee grounds were the best choice because they were waste and the cost of their preparation is low. Table 5 presented a list of adsorbents derived from renewable raw materials described in the literature. Among them, only β-cyclodextrin modified electrospinning fibers had q_{max} values at the same level, when using a sorbent concentration twice as high. All our β-cyclodextrin materials maintained a constant sorption capacity in the next five cycles, while the fibers lose 20% after four cycles.

3.2.4. Thermodynamic analysis

The thermodynamic parameters obtained from Eq. (2)–(4) provided supplementary information on the adsorption process (Table 5). The obtained positive values of ΔH° for each material meant that the processes were endothermic and proceeded with energy absorption. The most endothermic processes were those in which both dye and water are retained in the structure of the material. This phenomenon was accompanied by structural changes in the adsorbent resulting, inter alia, from an increase in volume. Cellulose modification significantly reduced the interaction with water, which was reflected in the reduction of the needed energy. Negative ΔG° values point to spontaneous and thermodynamically favorable processes as well as a high affinity of the adsorbate for the adsorbent (Bergmann and Machado, 2015). Positive values of ΔS° specified a high preference of the adsorbate molecules on the adsorbent surface. The highest values of ΔS° were determined for systems with structural changes (Lima et al., 2019).

3.2.5. Effect of pH salts, and humic acids on removal efficiency

The pHof a solution often has a significant impact on the adsorption efficiency of contaminants present in solutions, particularly during the treatment of industrial wastewater, which is sometimes extremely acidic or alkaline. In studies of the sorption process, CV solutions with pH ranging from 2 to 11 were used (Fig. 7a). In each case, a significantly lower dye removal efficiency was observed for pH= 2 of 9.3% (CC), 38% (CTCD), 43%(CGC), 48% (CG), 52% (CD-1), 54% (CT), and 55% (Cd-2).

Crystal violet is an alkaline dye containing three nitrogen atoms. Of the three salts, two are stable at very low pH while the third is even in alkaline media (Fig. 7b) (Adams et al., 1914). Thus, in a solution at pH2 there are organic cations (2.5 10^{-5} mol L^{-1}), protons (0.01 mol L^{-1}), an equivalent amount of chloride ions and a sorbent. The surface of the material regardless of the pHof the solution can be neutral, positively or negatively charged (Liu et al., 2020; Fröhlich et al., 2019; Streit et al., 2021). Very often the charge is the driving force of the adsorption process. In the system under consideration, if it is negative, electrostatic attraction of cations will occur very quickly. The concentration of protons is 400 times higher than that of organics. In addition, protons are small, light and very mobile, so they reach the surface of the adsorbent first. If the surface of the material is positive, the first interaction that will occur will be electrostatic repulsion toward the cations present there and attraction of chloride anions. The surface of the CC is consistently negative in the acidic range up to pH= 5.6. As the hydrogen ion concentration decreases, there is a slow increase in the degree of CV removal from 25% for pH 3, 49% for pH 4 and 88% for pH 5 for which we finally have a predominance of organic cations. The CTCD surface is also negative in acidic media but unlike CC it has two additional structural elements namely: aromatic and cyclodextrin rings, which are not attractive to protons but are to the dye which explains the better removal rate of 38% for pH 2 and 47% for pH 3. Positive surface charge (for example, CT and CD-1) in the low pHrange is less of a hindrance to the adsorption process. It is not excluded that the dye is adsorbed as an ion pair and not as a free cation, which significantly nullifies the ecetrostatic repulsion. Less processed CG and CGC materials contain acidic and alkaline components that buffer the pH of the environment to some extent, so the degree of dye removal is much higher compared to crystalline cellulose in pH 2. In a neutral environment, the dye removal efficiency is high and ranges from 92% to 98%. Undoubtedly, the dye in the cationic form (pKa = 8.64) is involved in the interaction with the material surface. A further increase in pH no longer has such a significant effect on the process.

The effect of salt by adding sodium or calcium chloride was also investigated, using rather high concentrations found in dye-house effluents (Fig. 7c) (Dutta et al., 2021). Among the seven materials, as many as six can successfully work in conditions of high salinity. The exception was microcrystalline cellulose. The presence of calcium ions in a lower concentration also negatively influenced the sorption capacity of CT, CTCD, and CD-1 and CD-2. Perhaps it was related to the easier migration of ions to mesopores and their filling. However, the biggest problem was humic acids present in high concentration, which happens in the case of surface water (Rodrigues et al., 2009; Tungsudjawong et al., 2018; Zhang et al., 2020). In this case, the degree of CV removal from the model wastewater was reduced by half for CC, CT, CTCD, and CD-1 (Fig. 7b). Nevertheless, these are only two-component solutions,

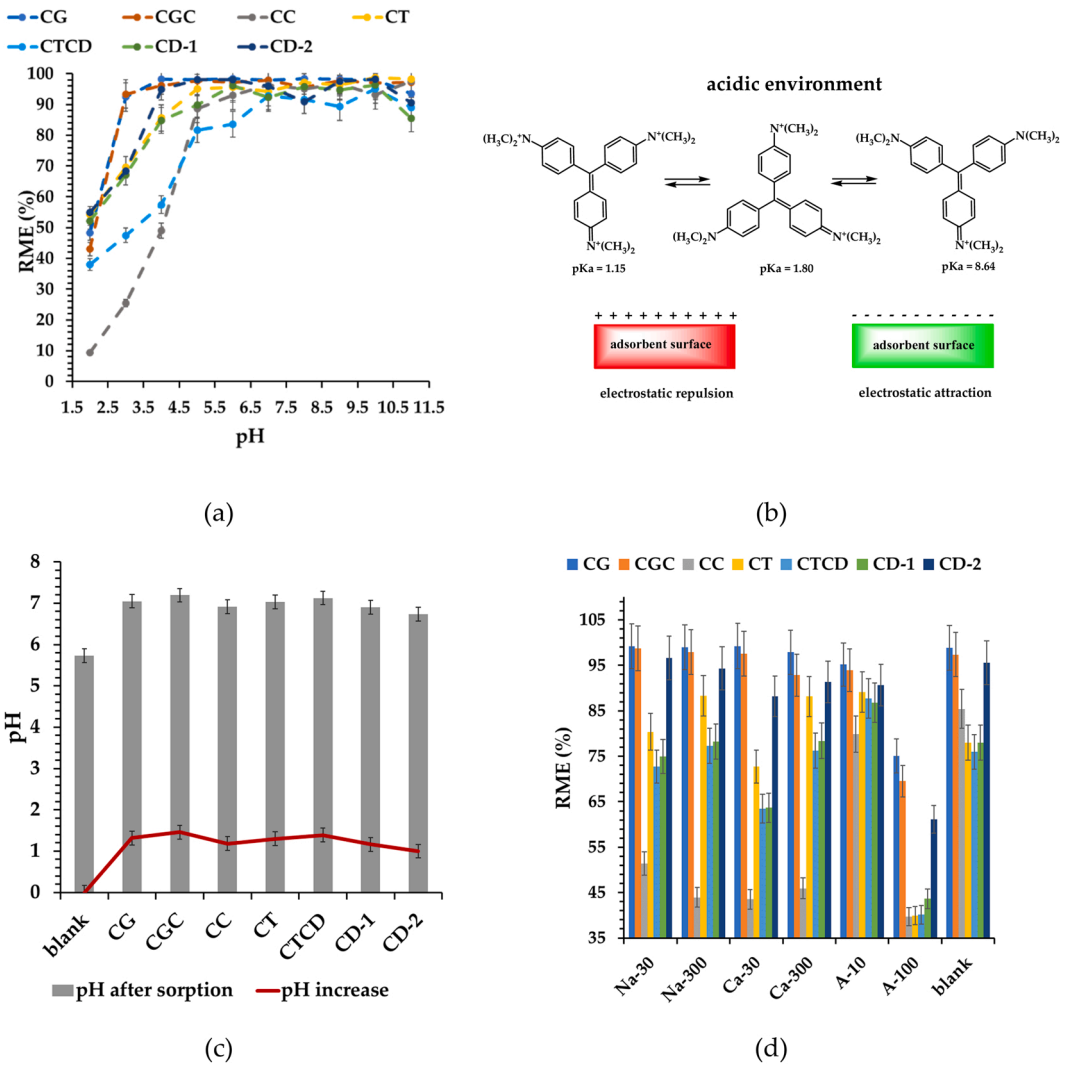

Fig. 7. Effect of (a) pH (b) Possible interactions of the adsorbent surface with the dye, (c) adsorption on the change of the pHof the solution; (d) salts and humic acids concentration on adsorption of CV (C_{CV} = 10.20 mg L^{-1}, pH= 5.7, m_{sor}= 10 mg) by sorbents ($t_{contact}$ = 20 min). Na-30 and Na-300 (C_{NaCl} = 76.05 mg L^{-1}; C_{NaCl} = 760.50 mg L^{-1}); Ca-30 and Ca-300 (C_{CaCl2} = 83.25 mg L^{-1}; C_{CaCl2} = 832.50 mg L^{-1}); A-10 and A-100 ($C_{humic\ acids}$ = 10 mg L^{-1}; $C_{humic\ acids}$ = 100 mg L^{-1}).

containing salt and CV or humic acids and CV. The matrix of real wastewater was much richer, which, paradoxically, may give a completely different effect on the dye sorption process.

3.2.6. *Environmental applications*

In environmental research, treated sewage from municipal sewage treatment plant containing organic and inorganic compounds in dissolved and suspended form was used. This choice was dictated by the use of a matrix that allows to simulate the situation when sewage treatment plants leave sewage containing undecomposed dyes (Fig. 1). So, the sewage was used to prepare dye solutions (Table S11). The results were compared with those obtained in model systems (Fig. 8.), not finding a very significant influence of the matrix on the sorption capacity of the materials, except for the CC-BP system. In this case, when the solvent was water, BP did not sorption at all. All materials show a much greater affinity for cationic dyes. The removal rate was high, ranging from 72% for the CG-BG system to 98.9% for the CD-2-BT system. Among the anionic dyes, CTC is the best sorbent for CG (RME = 77.8%). These preliminary results as well as high values of the maximum sorption capacity predicted the use of the cheapest adsorbent, i.e. CG, as a filling of actual filters supporting the process of wastewater treatment containing dyes and other organic compounds.

3.2.7. *Regenerative experiments*

An integral part of the sorption treatment process is the regeneration step, which is often a significant component of the total cost of the process and waste generation (Alzate-Sánchez et al., 2019, 2018; Menkiti and Aniagor, 2018). Seven sorbents were used for the tests, characterized by a different affinity for the CV, and thus the degree of difficulty in removing it from the surface during regeneration. For this purpose, methanol was used in which the CV is perfectly soluble. Methanol, on the other hand, is a cheap solvent, with a low boiling point and does not form an azeotrope with water, which considerably reduces the cost of a unit operation. As shown in Scheme 2, the most difficult was CC and CT regenerations (Usman et al., 2021). This process was the most efficient in the case of the low-cost CG, but it was less effective for CV removal in subsequent repetitions similar to CC (Lafi et al., 2014; Marincas et al., 2016). The opposite situation was observed for CD-containing materials (Skwierawska et al., 2021). This result was probably due to the materials' ability to remember the shape of the complexed dye after the second repetition (Xia et al., 2020). Spontaneous preorganization will remain intact during subsequent applications (Fig. 9a.).

All sorbents presented in this work were oligomers or polymers of D-glucose, so theoretically they should not have a negative impact on the natural environment during disposal in a manner similar to agricultural

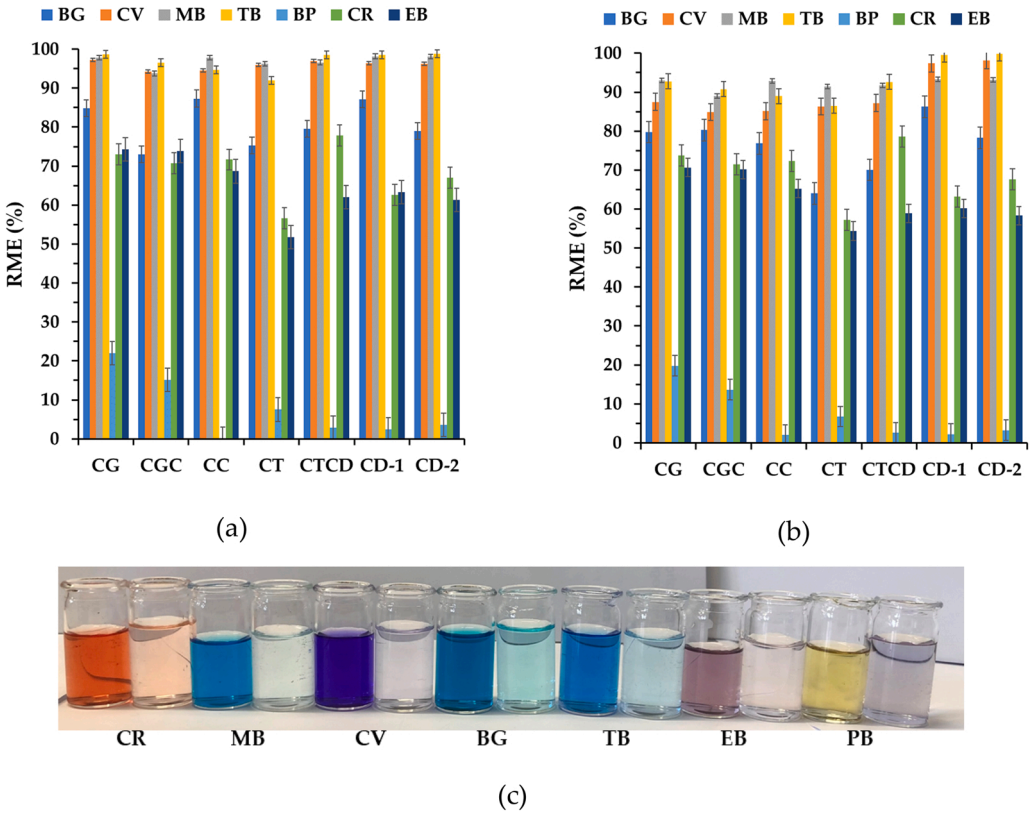

Fig. 8. The average efficiency of dyes (C_{dye} = 0.025 mmol L^{-1}, m_{sor}= 10 mg) removal from: (a) synthetic wastewater; (b) effluents; (c) Photo showing dye solutions before and after adsorption on CG.

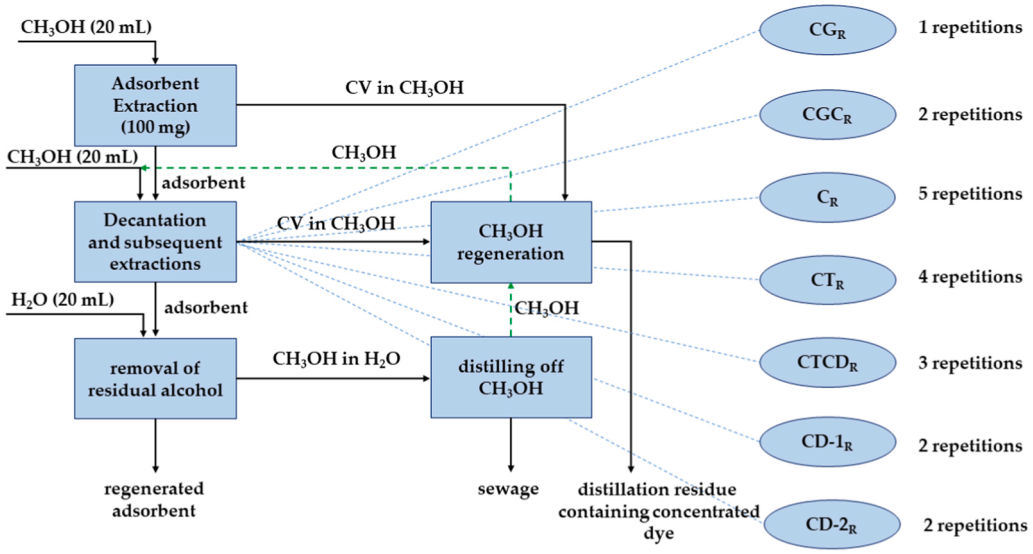

Scheme 2. A simplified schematic diagram of the adsorbent regeneration process.

waste (Afriliana et al., 2021). For this purpose, another experiment was carried out using mash obtained from baker's yeast and adsorbents after the fifth regeneration cycle (Table S12 and Table S13). The materials and mash were suspended in CV solution in the wastewater. After five days of the experiment, the materials were centrifuged and the COD and pH of the supernatants were determined by comparing them with the blank containing only yeast and sewage. In the case of CG, CD-1, and CD-2, the pH of the supernatants decreased to 2. The COD parameter decreased in each case in the range from 29% (CG) to 40.5% (CC) (Chen and Jin, 2006). In the first case, the color intensity of the supernatant was increasing with time (Fig. 9d). Appropriate types of yeast are used in the production of coffee, which in itself was an excellent breeding ground for microorganisms (Ruta and Farcasanu, 2021). It is also important that yeast greatly facilitates the removal of dye from the surface of the sorbent. One-time extraction with methanol enabled the quantitative removal of CV from the surface of each sorbent (Fig. 9e.) (Table S5).

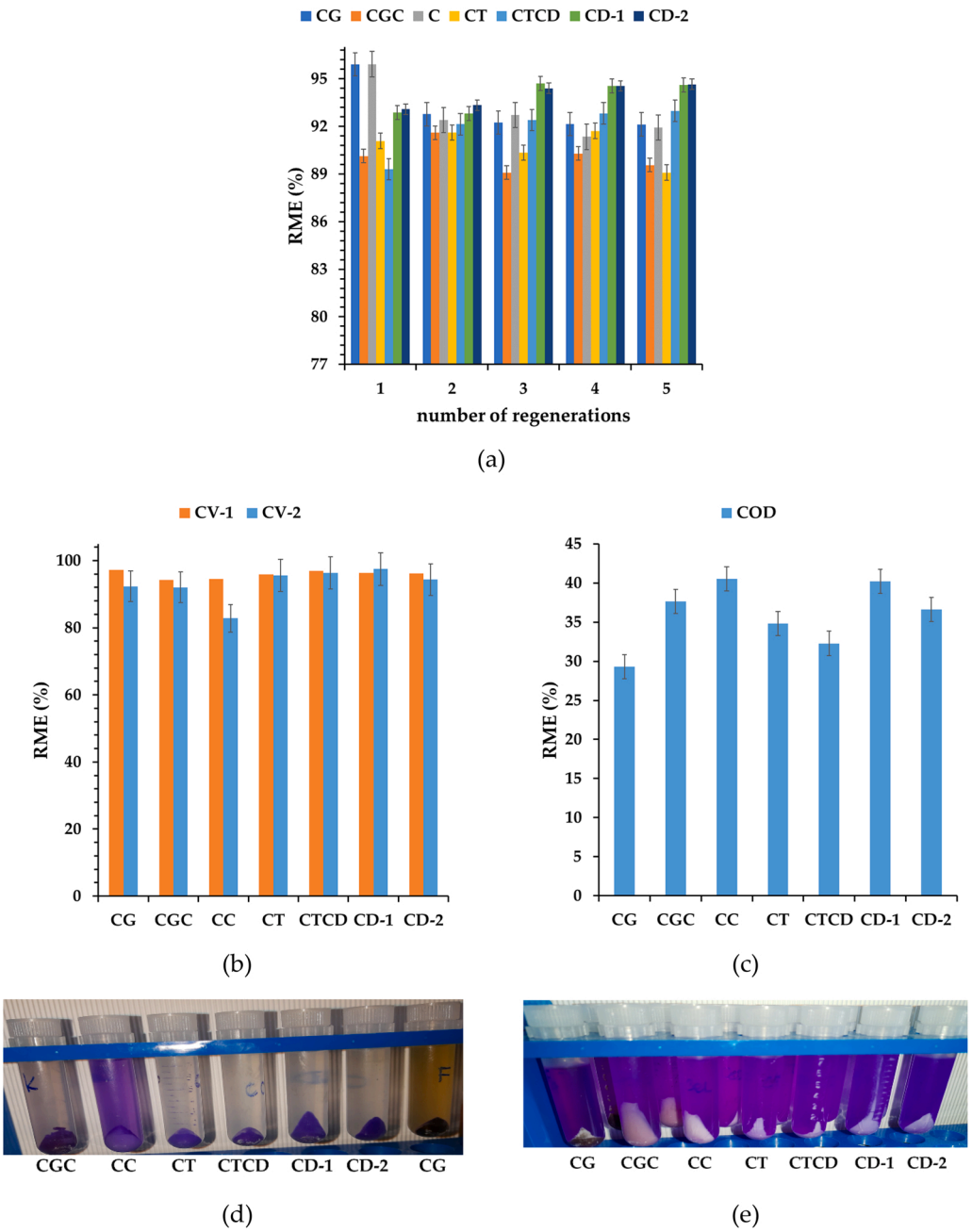

Fig. 9. (a) The average efficiency of CV (C_{CV} = 10.20 mg L^{-1}, m_{sor}= 10 mg) removal by sorbents after consecutive regeneration cycles; (b) The effects of CV removal from effluents containing yeasts; (c) The effects of yeasts on COD removal from effluents; (d) C-1, CV solution in tap water (C_{CV} = 10.20 mg L^{-1}, m_{sor}= 50 mg), C-2, CV solution in effluents (C_{CV} = ^{1}0.20 mg L^{-1}, m_{sor}= 50 mg, C_{yeast} = 1 g L^{-1}).

3.2.8. *Adsorption mechanism*

The main mechanism of dye sorption was based on the formation of hydrogen bonds and van der Waals interactions. The best example was CC which had a very ordered microcrystalline structure. A significant number of hydroxyl groups form hydrogen bonds. During sorption, they are partially destroyed in favor of new fibers connecting with the dye. The process was endothermic, but the resulting system provided a greater degree of disorder. The obtained energy minimum prevented the destruction of the new structure, hence the greatest difficulties with dye desorption. Cross-linking CC with toluene-2,4-di-isocyanate formed an amphiphilic system. The hydrophobic groups had the capacity to form hydrogen bonds, but the hydrophobic aromatic rings significantly reduced the wettability and thus the amount of water retained. Consequently, less energy must be supplied to the system during the sorption of the dye, which interacted with the surface not only through hydrogen bonds and van der Waals forces but also through π-π relations. As a result, the amount of retained dye was increased. Nevertheless, the introduction of spatial elements (aromatic rings) and groups competing in the formation of hydrogen bonds (urethane groups) facilitates desorption. The influence of other groups becomes apparent during CV sorption by CG and CGC. Probably, in this case, additional salts were formed by the reaction of the carboxyl and amino groups. CTCD was the system with the greatest potential to interact with dyes, as it is a structure composed of fibers and macrocycles linked together by TDI. Interactions intensifying during sorption were the sum of those described for CT and supramolecular ones. The latter allowed for better matching of the dye molecule to the sorbent structure. Additionally, the process gained selectivity. Forming supramolecular complexes forced

the preorganization of the material, which allowed for a better adjustment of the structure of the guest to the host. The new order facilitated sorption and desorption at the same time. The last two materials were made of cross-linked CD. The use of two different solvents had a significant impact on the physicochemical properties. The CD-1 kept the most CVs among the discussed above. The amount of embedded CD, assuming the formation of a 1: 1 complex, will only complex 179.73 mg g^{-1}, which meant that the residual amount was retained in the remaining structural elements of the network. Likewise, in the case of CD-2, which was obtained by reactions also allowing the condensation of secondary hydroxyl groups. A more random substitution led to a polymer in which a structurally distinct network connecting the CD torus also participates in sorption.

4. Conclusions

The paper presents a holistic approach to the sorption process carried out with the use of natural and semi-natural resources. Attention was drawn to the paradox resulting from the amount of generated wastewater in the case of using renewable raw materials and their lack of organic synthesis. The significant influence of the solvent and the cross-linking agents on the properties of the polymer as well as the significant share of hydroxyl groups in the structure of sorbents was demonstrated. Characterization analysis (TG / DTA, FTIR, EA, SEM) showed that the cellulose-containing materials are partially crystalline and partially amorphous. The degree of substitution of dehydroxyglucose monomers in chemically modified materials was in each case close to one, and the CD content is up to 50%. The materials were mesoporous. The CGC additionally contained macropores. Sorbents retained water to varying degrees, among them the most CGC (3 g g^{-1}). Materials in solutions with different pH achieve a point charge of zero, therefore a cationic dye was selected for the study. The results showed that CG, CGC, and CD-2 are the least sensitive to pH and can work efficiently in the range from 4 to 11. Kinetic and isothermal studies have shown that CV adsorption takes place on a relatively homogeneous surface. The dye adsorption by CG and CGC followed the pseudo-second model, while in the remaining cases it followed the pseudo-first model. The data on the material adsorption equilibria fit well with the two Langmuir and Sips models. The determined values of the maximum adsorption capacity for all materials were very high and exceed the value of 1000 mg g^{-1}.

All materials effectively remove other cationic dyes from wastewater. The materials after the sorption of impurities can be regenerated under mild conditions and used at least five times. Waste sorbents are not toxic to yeasts and can be decomposed during composting assisted with this type of microorganisms. The yeast enables the quantitative desorption of the dye in the first step. From the point of availability of the raw material, the possibility of its final decomposition by composting, ordinary Arabica coffee grounds are the best choice. On the other hand, when assessing the stability during regeneration and even the increase in sorption capacity, as a result of probably remembering the shape of pollutants, materials containing CD win the race.

Environmental implication

Adsorption is one of the basic processes for removing organic pollutants from wastewater. Nevertheless, a serious disadvantage of this method is the issue of managing the used adsorbents. The new idea is to use renewable raw materials in a native or processed form with the assumption of their potential biodegradation. These types of adsorbents can be obtained from plant waste, which significantly reduces the cost of the process. It also gives the opportunity to make better use of native waste. The used sorbents can be composted and thus transformed into organic fertilizer, which solves the issue of storage.

CRediT authorship contribution statement

Anna Skwierawska: Conceptualization, Methodology, Investigation, Formal analysis, Validation, Writing - original draft, Visualization, Writing - review & editing. **Monika Bliźniewska**: Investigation, Writing - review & editing. **Kinga Muza**: Investigation, Writing - review & editing. **Agnieszka Nowak**: Investigation, Writing - review & editing. **Dominika Nowacka**: Validation, Writing - review & editing, **Shan E Zehra Syeda:** Investigation, Writing - review & editing, **Muhammad Shahzeb Khan:** Investigation, Writing - review & editing, **Bogusława Łęska:** Funding acquisition, Writing - review & editing.

Declaration of Competing Interest

The authors declare that they have no known competing financial interests or personal relationships that could have appeared to influence the work reported in this paper.

Data availability

No data was used for the research described in the article.

Acknowledgements

The authors are grateful for financial support provided by Gdańsk University of Technology, SB 035376.

Appendix A. Supporting information

Supplementary data associated with this article can be found in the online version at doi:10.1016/j.jhazmat.2022.129588.

References

Abu-Danso, E., Bagheri, A., Bhatnagar, A., 2019. Facile functionalization of cellulose from discarded cigarette butts for the removal of diclofenac from water. Carbohydr. Polym. 219, 46–55. https://doi.org/10.1016/j.carbpol.2019.04.090.

Adams, E.Q., Rosenstein, L., Ziegel, H., 1914. potential dif- 624, 1363–1371.

Afriliana, A., Hidayat, E., Mitoma, Y., Masuda, T., Harada, H., 2021. Studies on composting spent coffee grounds by Aspergillus sp and Penicillium sp in aerobic static batch temperature control. J. Agric. Chem. Environ. 10, 91–112. https://doi.org/10.4236/jacen.2021.101007.

Ahalya, N., Chandraprabha, M.N., Kanamadi, R.D., Ramachandra, T.V., 2014. Adsorption of fast green on to coffee husk. J. Chem. Eng. Res. 2, 201–207.

Åkerholm, M., Hinterstoisser, B., Salmén, L., 2004. Characterization of the crystalline structure of cellulose using static and dynamic FT-IR spectroscopy. Carbohydr. Res. 339, 569–578. https://doi.org/10.1016/j.carres.2003.11.012.

Alzate-Sánchez, D.M., Ling, Y., Li, C., Frank, B.P., Bleher, R., Howard Fairbrother, D., Helbling, D.E., Dichtel, W.R., 2018. β-Cyclodextrin polymers on microcrystalline cellulose as a granular media for organic micropollutant removal from water. ChemRxiv 60208, 1–16. https://doi.org/10.26434/chemrxiv.7471508.v1.

Alzate-Sánchez, D.M., Ling, Y., Li, C., Frank, B.P., Bleher, R., Fairbrother, D.H., Helbling, D.E., Dichtel, W.R., Howard Fairbrother, D., Helbling, D.E., Dichtel, W.R., 2019. β-Cyclodextrin polymers on microcrystalline cellulose as a granular media for organic micropollutant removal from water. ACS Appl. Mater. Interfaces 11, 8089–8096. https://doi.org/10.1021/acsami.8b22100.

Anne, J.M., Boon, Y.H., Saad, B., Miskam, M., Yusoff, M.M., Shahriman, M.S., Zain, N.N. M., Lim, V., Raoov, M., 2018. b-Cyclodextrin conjugated bifunctional isocyanate linker polymer for enhanced removal of 2,4-dinitrophenol from environmental waters. R. Soc. Open Sci. 5. https://doi.org/10.1098/rsos.180942.

Ayalew, A.A., Aragaw, T.A., 2020. Utilization of treated coffee husk as low-cost biosorbent for adsorption of methylene blue. Adsorpt. Sci. Technol. 38, 205–222. https://doi.org/10.1177/0263617420920516.

Badruddoza, A.Z.M., Bhattarai, B., Suri, R.P.S., 2017. Environmentally friendly β-cyclodextrin-ionic liquid polyurethane-modified magnetic sorbent for the removal of PFOA, PFOS, and Cr(VI) from water. ACS Sustain. Chem. Eng. 5, 9223–9232. https://doi.org/10.1021/acssuschemeng.7b02186.

Ballesteros, L.F., Teixeira, J.A., Mussatto, S.I., 2014. Chemical, functional, and structural properties of spent coffee grounds and coffee silverskin. Food Bioprocess Technol. 7, 3493–3503. https://doi.org/10.1007/s11947-014-1349-z.

Barrett, E.P., Joyner, L.G., Halenda, P.P., 1951. The determination of pore volume and area distributions in porous substances. I. Computations from nitrogen isotherms. J. Am. Chem. Soc. 73, 373–380. https://doi.org/10.1021/ja01145a126.

Bazzo, A., Adebayo, M.A., Dias, S.L.P., Lima, E.C., Vaghetti, J.C.P., de Oliveira, E.R., Leite, A.J.B., Pavan, F.A., 2016. Avocado seed powder: characterization and its

application for crystal violet dye removal from aqueous solutions. Desalin. Water Treat. 57, 15873–15888. https://doi.org/10.1080/19443994.2015.1074621.
Bello, O.S., Alao, O.C., Alagbada, T.C., Agboola, O.S., Omotoba, O.T., Abikoye, O.R., 2021. A renewable, sustainable and low-cost adsorbent for ibuprofen removal. Water Sci. Technol. 83, 111–122. https://doi.org/10.2166/wst.2020.551.
Bhadra, B.N., Ahmed, I., Kim, S., Jhung, S.H., 2017. Adsorptive removal of ibuprofen and diclofenac from water using metal-organic framework-derived porous carbon. Chem. Eng. J. 314, 50–58. https://doi.org/10.1016/j.cej.2016.12.127.
Boehm, H.P., 1966. Chemical identification of surface groups. Adv. Catal. 16, 179–274. https://doi.org/10.1016/S0360-0564(08)60354-5.
Börjesson, M.H., Ahlgren, E.O., 2015. Pulp and paper industry intelligence. IEA ETSAP - Technol. Brief. 107, 1–9.
Brännvall, E., 2009. Overview of pulp and paper processes. Pulping Chem. Technol. 1–11. https://doi.org/10.1515/9783110213423.
Brinchi, L., Cotana, F., Fortunati, E., Kenny, J.M., 2013. Production of nanocrystalline cellulose from lignocellulosic biomass: technology and applications. Carbohydr. Polym. 94, 154–169. https://doi.org/10.1016/j.carbpol.2013.01.033.
Brunauer, S., Emmett, P.H., Teller, E., 1938. Adsorption of gases in multimolecular layers. J. Am. Chem. Soc. 60, 309–319. https://doi.org/10.1021/ja01269a023.
Bulut, Y., Aydin, H., 2006. A kinetics and thermodynamics study of methylene blue adsorption on wheat shells. Desalination 194, 259–267. https://doi.org/10.1016/j.desal.2005.10.032.
Cadena, P.G., Oliveira, E.C., Araújo, A.N., Montenegro, M.C.B.S.M., Pimentel, M.C.B., Lima Filho, J.L., Silva, V.L., 2009. Simple determination of deoxycholic and ursodeoxycholic acids by phenolphthalein-β-cyclodextrin inclusion complex. Lipids 44, 1063–1070. https://doi.org/10.1007/s11745-009-3353-z.
Chalker-scott, L., 2021. Using coffee grounds in gardens and landscapes.
Chen, H., Jin, S., 2006. Effect of ethanol and yeast on cellulase activity and hydrolysis of crystalline cellulose. Enzym. Microb. Technol. 39, 1430–1432. https://doi.org/10.1016/j.enzmictec.2006.03.027.
Chen, J., Pu, Y., Wang, C., Han, J., Zhong, Y., Liu, K., 2018. Synthesis of a novel nanosilica-supported poly β-cyclodextrin sorbent and its properties for the removal of dyes from aqueous solution. Colloids Surf. A Physicochem. Eng. Asp. 538, 808–817. https://doi.org/10.1016/j.colsurfa.2017.11.048.
Ching, C., Klemes, M.J., Trang, B., Dichtel, W.R., Helbling, D.E., 2020. β-Cyclodextrin polymers with different cross-linkers and ion-exchange resins exhibit variable adsorption of anionic, zwitterionic, and nonionic PFASs. Environ. Sci. Technol. 54, 12693–12702. https://doi.org/10.1021/acs.est.0c04028.
Ding, S., Liu, P., Zhang, S., Gao, C., Wang, F., Ding, Y., Yang, M., 2020. Crosslinking of β-cyclodextrin and combining with ammonium polyphosphate for flame-retardant polypropylene. J. Appl. Polym. Sci. 137, 1–12. https://doi.org/10.1002/app.48320.
Dutta, S., Gupta, B., Srivastava, S.K., Gupta, A.K., 2021. Recent advances on the removal of dyes from wastewater using various adsorbents: a critical review. Mater. Adv. 2, 4497–4531. https://doi.org/10.1039/d1ma00354b.
Elgarahy, A.M., Elwakeel, K.Z., Elshoubaky, G.A., Mohammad, S.H., 2019. Untapped sepia shell–based composite for the sorption of cationic and anionic dyes. Water Air Soil Pollut. 230. https://doi.org/10.1007/s11270-019-4247-1.
Elgarahy, A.M., Elwakeel, K.Z., Mohammad, S.H., Elshoubaky, G.A., 2021. A critical review of biosorption of dyes, heavy metals and metalloids from wastewater as an efficient and green process. Clean. Eng. Technol. 4, 100209 https://doi.org/10.1016/j.clet.2021.100209.
Elgarahy, Ahmed M., Elwakeel, K.Z., Elshoubaky, G.A., Mohammad, S.H., 2019. Microwave-accelerated sorption of cationic dyes onto green marine algal biomass. Environ. Sci. Pollut. Res. 26, 22704–22722. https://doi.org/10.1007/s11356-019-05417-2.
Elwakeel, K.Z., 2009. Removal of Reactive Black 5 from aqueous solutions using magnetic chitosan resins. J. Hazard. Mater. 167, 383–392. https://doi.org/10.1016/j.jhazmat.2009.01.051.
Elwakeel, K.Z., Elgarahy, A.M., Elshoubaky, G.A., Mohammad, S.H., 2020. Microwave assist sorption of crystal violet and Congo red dyes onto amphoteric sorbent based on upcycled Sepia shells 03 Chemical Sciences 0306 Physical Chemistry (incl. Structural). J. Environ. Health Sci. Eng. 18, 35–50. https://doi.org/10.1007/s40201-019-00435-1.
Elwakeel, K.Z., Elgarahy, A.M., Al-Bogami, A.S., Hamza, M.F., Guibal, E., 2021a. 2-Mercaptobenzimidazole-functionalized chitosan for enhanced removal of methylene blue: Batch and column studies. J. Environ. Chem. Eng. 9, 105609 https://doi.org/10.1016/j.jece.2021.105609.
Elwakeel, K.Z., Elgarahy, A.M., Guibal, E., 2021b. A biogenic tunable sorbent produced from upcycling of aquatic biota-based materials functionalized with methylene blue dye for the removal of chromium(VI) ions. J. Environ. Chem. Eng. 9, 104767 https://doi.org/10.1016/j.jece.2020.104767.
Erdös, M., Hartkamp, R., Vlugt, T.J.H., Moultos, O.A., 2020. Inclusion complexation of organic micropollutants with β-cyclodextrin. J. Phys. Chem. B 124, 1218–1228. https://doi.org/10.1021/acs.jpcb.9b10122.
Ferrero, F., 2007. Dye removal by low cost adsorbents: Hazelnut shells in comparison with wood sawdust. J. Hazard. Mater. 142, 144–152. https://doi.org/10.1016/j.jhazmat.2006.07.072.
Ferro, M., Castiglione, F., Punta, C., Melone, L., Panzeri, W., Rossi, B., Trotta, F., Mele, A., 2014. Anomalous diffusion of ibuprofen in cyclodextrin nanosponge hydrogels: an HRMAS NMR study. Beilstein J. Org. Chem. 10, 2715–2723. https://doi.org/10.3762/bjoc.10.286.
Freundlich, H.M.F., 1906. Uber die adsorption in Lasugen. J. Phys. Chem. 57.
Fröhlich, A.C., Foletto, E.L., Dotto, G.L., 2019. Preparation and characterization of NiFe2O4/activated carbon composite as potential magnetic adsorbent for removal of ibuprofen and ketoprofen pharmaceuticals from aqueous solutions. J. Clean. Prod. 229, 828–837. https://doi.org/10.1016/j.jclepro.2019.05.037.
Futalan, C.M., Kim, J., Yee, J.J., 2019. Adsorptive treatment via simultaneous removal of copper, lead and zinc from soil washing wastewater using spent coffee grounds. Water Sci. Technol. 79, 1029–1041. https://doi.org/10.2166/wst.2019.087.
Garg, A., Chopra, L., 2022. Dye Waste: A significant environmental hazard. Mater. Today Proc. 48, 1310–1315. https://doi.org/10.1016/j.matpr.2021.09.003.
Goel, A., Nene, S.N., 1995. Modifications in the phenolphthalein method for spectrophotometric estimation of beta cyclodextrin. Starch - Stärke 47, 399–400. https://doi.org/10.1002/star.19950471006.
Harshananda, T.N., Ayisha, T.M., Janani Priyanka, P.R., Dildar Mather, K.N., R.V.P, 2020. Removal of colour from textile effluent by adsorption using banana stem and coffee husk: a Review. IOSR J. Mech. Civ. Eng. 17, 32–41. https://doi.org/10.9790/1684-1704013241.
Hemine, K., Skwierawska, A., Kernstein, A., Kozłowska-Tylingo, K., 2020. Cyclodextrin polymers as efficient adsorbents for removing toxic non-biodegradable pimavanserin from pharmaceutical wastewaters. Chemosphere 250. https://doi.org/10.1016/j.chemosphere.2020.126250.
Hoti, G., Caldera, F., Cecone, C., Pedrazzo, A.R., Anceschi, A., Appleton, S.L., Monfared, Y.K., Trotta, F., 2021. Effect of the cross-linking density on the swelling and rheological behavior of ester-bridged β-cyclodextrin nanosponges. Materials 14, 1–20. https://doi.org/10.3390/ma14030478.
Hu, X., Xu, G., Zhang, H., Li, M., Tu, Y., Xie, X., Zhu, Y., Jiang, L., Zhu, X., Ji, X., Li, Y., Li, A., 2020. Multifunctional β-cyclodextrin polymer for simultaneous removal of natural organic matter and organic micropollutants and detrimental microorganisms from water. ACS Appl. Mater. Interfaces 12, 12165–12175. https://doi.org/10.1021/acsami.0c00597.
Huang, H., Wang, J., Fan, Y., Tao, S., 2012. Adsorption behavior of β-Cyclodextrin polymer to phenol in aqueous solution. Adv. Mater. Res. 554–556, 177–180. https://doi.org/10.4028/www.scientific.net/AMR.554-556.177.
Huang, Q., Chai, K., Zhou, L., Ji, H., 2020. A phenyl-rich β-cyclodextrin porous crosslinked polymer for efficient removal of aromatic pollutants: insight into adsorption performance and mechanism. Chem. Eng. J. 387, 124020 https://doi.org/10.1016/j.cej.2020.124020.
Ibiyinka, O., Akinwumi Oluwafemi, A., Adebayo O, O., Olugbenga Kayode, P., 2021. Comparative study of chemical composition and evaluation of the In-Vitro antioxidant capacity of unripe and ripe banana species (Musa Sapientum) biowastes. Int. J. Agric. Sci. Food Technol. 7, 061–066. https://doi.org/10.17352/2455-815x.000089.
Jia, S., Tang, D., Peng, J., Sun, Z., Yang, X., 2019. β-Cyclodextrin modified electrospinning fibers with good regeneration for efficient temperature-enhanced adsorption of crystal violet. Carbohydr. Polym. 208, 486–494. https://doi.org/10.1016/j.carbpol.2018.12.075.
Kalemelawa, F., Nishihara, E., Endo, T., Ahmad, Z., Yeasmin, R., Tenywa, M.M., Yamamoto, S., 2012. An evaluation of aerobic and anaerobic composting of banana peels treated with different inoculums for soil nutrient replenishment. Bioresour. Technol. 126, 375–382. https://doi.org/10.1016/j.biortech.2012.04.030.
Karoyo, A.H., Yang, J., Wilson, L.D., 2018. Cyclodextrin-based polymer-supported bacterium for the adsorption and in-situ biodegradation of phenolic compounds. Front. Chem. 6. https://doi.org/10.3389/fchem.2018.00403.
Katheresan, V., Kansedo, J., Lau, S.Y., 2018. Efficiency of various recent wastewater dye removal methods: a review. J. Environ. Chem. Eng. 6, 4676–4697. https://doi.org/10.1016/j.jece.2018.06.060.
Kim, M.S., Kim, J.G., 2020. Adsorption characteristics of spent coffee grounds as an alternative adsorbent for cadmium in solution. Environ. - MDPI 7, 1–12. https://doi.org/10.3390/environments7040024.
Kim, T.J., Kim, B.C., Lee, H.S., 1997. Production of cyclodextrin using raw corn starch without a pretreatment. Enzym. Microb. Technol. 20, 506–509. https://doi.org/10.1016/S0141-0229(96)00186-X.
Kyzas, G.Z., 2012. A decolorization technique with spent “Greek coffee” grounds as zero-cost adsorbents for industrial textile wastewaters. Materials 5, 2069–2087. https://doi.org/10.3390/ma5112069.
Lafi, R., ben Fradj, A., Hafiane, A., Hameed, B.H., 2014. Coffee waste as potential adsorbent for the removal of basic dyes from aqueous solution. Korean J. Chem. Eng. 31, 2198–2206. https://doi.org/10.1007/s11814-014-0171-7.
Langmuir, I., 1916. of the gas is absorbed in the charcoal structure, in accordance with the In conclusion, the writer wishes to express his thanks to the authorities facilities of the chemical laboratory of that institution for the purposes THE CONSTITUTION AND FUNDAMENTA 468.
Langmuir, I., 1917. The constitution and fundamental properties of solids and liquids. II. Liquids. 39, 1848–1906. https://doi.org/https://doi.org/10.1021/ja02254a006.
Lellis, B., Fávaro-Polonio, C.Z., Pamphile, J.A., Polonio, J.C., 2019. Effects of textile dyes on health and the environment and bioremediation potential of living organisms. Biotechnol. Res. Innov. 3, 275–290. https://doi.org/10.1016/j.biori.2019.09.001.
Leone, V.O., Pereira, M.C., Aquino, S.F., Oliveira, L.C.A., Correa, S., Ramalho, T.C., Gurgel, L.V.A., Silva, A.C., 2018. Adsorption of diclofenac on a magnetic adsorbent based on maghemite: experimental and theoretical studies. N. J. Chem. 42, 437–449. https://doi.org/10.1039/c7nj03214e.
Lessa, E.F., Nunes, M.L., Fajardo, A.R., 2018. Chitosan/waste coffee-grounds composite: an efficient and eco-friendly adsorbent for removal of pharmaceutical contaminants from water. Carbohydr. Polym. 189, 257–266. https://doi.org/10.1016/j.carbpol.2018.02.018.
Li, W., Cai, G., Zhang, P., 2019. A simple and rapid Fourier transform infrared method for the determination of the degree of acetyl substitution of cellulose nanocrystals. J. Mater. Sci. 54, 8047–8056. https://doi.org/10.1007/s10853-019-03471-2.
Lima, E.C., Hosseini-Bandegharaei, A., Moreno-Piraján, J.C., Anastopoulos, I., 2019. A critical review of the estimation of the thermodynamic parameters on adsorption equilibria. Wrong use of equilibrium constant in the Van’t Hoof equation for

calculation of thermodynamic parameters of adsorption. J. Mol. Liq. 273, 425–434. https://doi.org/10.1016/j.molliq.2018.10.048.
Liu, D., Huang, Z., Li, M., Li, X., Sun, P., Zhou, L., 2020. Construction of magnetic bifunctional β-cyclodextrin nanocomposites for adsorption and degradation of persistent organic pollutants. Carbohydr. Polym. 230. https://doi.org/10.1016/j.carbpol.2019.115564.
Liu, H.-J., Feng, Z.-M., Cao, S., Li, Y., 2016. Improving the production of cyclodextrins from the Paenibacillus polymyxa in Bacillus subtilis 498–504. https://doi.org/10.1142/9789813200470_0059.
Liu, Q., 2020. Pollution and treatment of dye waste-water. IOP Conf. Ser. Earth Environ. Sci. 514. https://doi.org/10.1088/1755-1315/514/5/052001.
Loulidi, I., Boukhlifi, F., Ouchabi, M., Amar, A., Jabri, M., Kali, A., Hadey, C., 2021. Assessment of untreated coffee wastes for the removal of chromium (VI) from aqueous medium. Int. J. Chem. Eng. 2021. https://doi.org/10.1155/2021/9977817.
Luo, H., Zhang, Y., Xie, Y., Li, Y., Qi, M., Ma, R., Yang, S., Wang, Y., 2019. Iron-rich microorganism-enabled synthesis of magnetic biocarbon for efficient adsorption of diclofenac from aqueous solution. Bioresour. Technol. 282, 310–317. https://doi.org/10.1016/j.biortech.2019.03.028.
Marincas, O., Floare-Avram, V., Feher, I., Lazăr, D., Voica, C., Grosu, I., 2016. Inexpensive adsorbents derived from coffee grounds for the treatment of wastewater. Anal. Lett. 49, 2659–2670. https://doi.org/10.1080/00032719.2015.1125913.
Martín, J., Orta, M., del, M., Medina-Carrasco, S., Santos, J.L., Aparicio, I., Alonso, E., 2019. Evaluation of a modified mica and montmorillonite for the adsorption of ibuprofen from aqueous media. Appl. Clay Sci. 171, 29–37. https://doi.org/10.1016/j.clay.2019.02.002.
Menkiti, M.C., Aniagor, C.O., 2018. Parametric studies on descriptive isotherms for the uptake of crystal violet dye from aqueous solution onto lignin-rich adsorbent. Arab. J. Sci. Eng. 43, 2375–2392. https://doi.org/10.1007/s13369-017-2789-3.
Militao, I.M., Roddick, F.A., Bergamasco, R., Fan, L., 2021. Removing PFAS from aquatic systems using natural and renewable material-based adsorbents: a review. J. Environ. Chem. Eng. 9. https://doi.org/10.1016/j.jece.2021.105271.
Mohamed, M.H., Wilson, L.D., Pratt, D.Y., Guo, R., Wu, C., Headley, J.V., 2012. Evaluation of the accessible inclusion sites in copolymer materials containing β-cyclodextrin. Carbohydr. Polym. 87, 1241–1248. https://doi.org/10.1016/j.carbpol.2011.09.011.
Mohit, N., Agarwal, B., Porwal, A., Yadav, B., Dhannajay, K., 2014. Manufacturing of paper by sulphate (kraft) process. Int. J. Sci. Res. Rev. 3, 106–120.
Nelson, M.L., O'Connor, R.T., 1964. Relation of certain infrared bands to cellulose crystallinity and crystal lattice type. Part II. A new infrared ratio for estimation of crystallinity in celluloses I and II. J. Appl. Polym. Sci. 8, 1325–1341. https://doi.org/10.1002/app.1964.070080323.
Oh, S.Y., Yoo, D., Il, Shin, Y., Seo, G., 2005. FTIR analysis of cellulose treated with sodium hydroxide and carbon dioxide. Carbohydr. Res. 340, 417–428. https://doi.org/10.1016/j.carres.2004.11.027.
Oliveira, L.S., Franca, A.S., Alves, T.M., Rocha, S.D.F., 2008. Evaluation of untreated coffee husks as potential biosorbents for treatment of dye contaminated waters. J. Hazard. Mater. 155, 507–512. https://doi.org/10.1016/j.jhazmat.2007.11.093.
Pagalan, E., Sebron, M., Gomez, S., Salva, S.J., Ampusta, R., Macarayo, A.J., Joyno, C., Ido, A., Arazo, R., Moustafa, H., Guizani, C., Dufresne, A., Kyzas, G.Z., Hao, L., Wang, P., Valiyaveettil, S., Ballesteros, L.F., Teixeira, J.A., Mussatto, S.I., Kim, M.S., Kim, J.G., Sisti, L., Celli, A., Totaro, G., Cinelli, P., Signori, F., Lazzeri, A., Bikaki, M., Corvini, P., Ferri, M., Tassoni, A., Navarini, L., 2020. Adsorption characteristics of spent coffee grounds as an alternative adsorbent for cadmium in solution. Food Bioprocess Technology 7, 1–12. https://doi.org/10.1002/app.44498.
Pavan, F.A., Lima, E.C., Dias, S.L.P., Mazzocato, A.C., 2008. Methylene blue biosorption from aqueous solutions by yellow passion fruit waste. J. Hazard. Mater. 150, 703–712. https://doi.org/10.1016/j.jhazmat.2007.05.023.
Qin, P., Xu, X., Cai, Y., Bai, B., Wang, H., Suo, Y., 2017. Fabrication of phytic acid-modified wheat straw platform and its pH-responsive release performance for the pesticide imidacloprid. RSC Adv. 7, 32777–32785. https://doi.org/10.1039/c7ra04354f.
Queirós, C.S.G.P., Cardoso, S., Lourenço, A., Ferreira, J., Miranda, I., Lourenço, M.J.V., Pereira, H., 2020. Characterization of walnut, almond, and pine nut shells regarding chemical composition and extract composition. Biomas Convers. Biorefinery 10, 175–188. https://doi.org/10.1007/s13399-019-00424-2.
Rafatullah, M., Sulaiman, O., Hashim, R., Ahmad, A., 2010. Adsorption of methylene blue on low-cost adsorbents: a review. J. Hazard. Mater. 177, 70–80. https://doi.org/10.1016/j.jhazmat.2009.12.047.
Raimondo, M., Caracciolo, F., Cembalo, L., Chinnici, G., Pecorino, B., D'Amico, M., 2018. Making virtue out of necessity: managing the citrus waste supply chain for bioeconomy applications. Sustainability 10, 1–19. https://doi.org/10.3390/su10124821.
Rajput, K.N., Patel, K.C., Trivedi, U.B., 2016. β-cyclodextrin production by cyclodextrin glucanotransferase from an alkaliphile Microbacterium terrae KNR 9 using different starch substrates. Biotechnol. Res. Int. 2016, 1–7. https://doi.org/10.1155/2016/2034359.
Rodrigues, A., Brito, A., Janknecht, P., Proena, M.F., Nogueira, R., 2009. Quantification of humic acids in surface water: effects of divalent cations, pH, and filtration]. J. Environ. Monit. 11, 377–382. https://doi.org/10.1039/b811942b.
Ruta, L.L., Farcasanu, I.C., 2021. Coffee and yeasts: from flavor to biotechnology. Fermentation 7. https://doi.org/10.3390/fermentation7010009.
Saeed, A., Sharif, M., Iqbal, M., 2010. Application potential of grapefruit peel as dye sorbent: kinetics, equilibrium and mechanism of crystal violet adsorption. J. Hazard. Mater. 179, 564–572. https://doi.org/10.1016/j.jhazmat.2010.03.041.
Sathishkumar, P., Arulkumar, M., Ashokkumar, V., Mohd Yusoff, A.R., Murugesan, K., Palvannan, T., Salam, Z., Ani, F.N., Hadibarata, T., 2015. Modified phyto-waste Terminalia catappa fruit shells: a reusable adsorbent for the removal of micropollutant diclofenac. RSC Adv. 5, 30950–30962. https://doi.org/10.1039/c4ra11786g.
Scroll, P., For, D., 2012. Biological Agriculture & Horticulture: An International Journal for Sustainable Production Systems Decomposition of Crop Residues in Banana-Based Cropping Systems of 1–10.
Shahnaz, T., Vishnu Priyan, V., Pandian, S., Narayanasamy, S., 2021. Use of Nanocellulose extracted from grass for adsorption abatement of Ciprofloxacin and Diclofenac removal with phyto, and fish toxicity studies. Environ. Pollut. 268, 115494 https://doi.org/10.1016/j.envpol.2020.115494.
Shindhal, T., Rakholiya, P., Varjani, S., Pandey, A., Ngo, H.H., Guo, W., Ng, H.Y., Taherzadeh, M.J., 2021. A critical review on advances in the practices and perspectives for the treatment of dye industry wastewater. Bioengineered 12, 70–87. https://doi.org/10.1080/21655979.2020.1863034.
Sips, R., 1948. On the structure of a catalyst surface. J. Chem. Phys. 16, 490–495. https://doi.org/10.1063/1.1746922.
Sivarajasekar, N., Mohanraj, N., Sivamani, S., Prakash Maran, J., Ganesh Moorthy, I., Balasubramani, K., 2018. Statistical optimization studies on adsorption of ibuprofen onto Albizialebbeck seed pods activated carbon prepared using microwave irradiation. Mater. Today Proc. 5, 7264–7274. https://doi.org/10.1016/j.matpr.2017.11.394.
Skwierawska, A.M., Nowacka, D., Nowicka, P., Rosa, S., Kozłowska-Tylingo, K., 2021. Structural adaptive, self-separating material for removing ibuprofen from waters and sewage. Materials 14, 1–23. https://doi.org/10.3390/ma14247697.
Soares, S.F., Fernandes, T., Sacramento, M., Trindade, T., Daniel-da-Silva, A.L., 2019. Magnetic quaternary chitosan hybrid nanoparticles for the efficient uptake of diclofenac from water. Carbohydr. Polym. 203, 35–44. https://doi.org/10.1016/j.carbpol.2018.09.030.
Streit, A.F.M., Collazzo, G.C., Druzian, S.P., Verdi, R.S., Foletto, E.L., Oliveira, L.F.S., Dotto, G.L., 2021. Adsorption of ibuprofen, ketoprofen, and paracetamol onto activated carbon prepared from effluent treatment plant sludge of the beverage industry. Chemosphere 262. https://doi.org/10.1016/j.chemosphere.2020.128322.
Tomul, F., Arslan, Y., Kabak, B., Trak, D., Kendüzler, E., Lima, E.C., Tran, H.N., 2020. Peanut shells-derived biochars prepared from different carbonization processes: comparison of characterization and mechanism of naproxen adsorption in water. Sci. Total Environ. 726. https://doi.org/10.1016/j.scitotenv.2020.137828.
Trends, T., Younas, F., Mustafa, A., Ur, Z., Farooqi, R., Wang, X., Younas, S., Mohy-ud-din, W., Hameed, M.A., Abrar, M.M., Maitlo, A.A., Noreen, S., Hussain, M.M., 2021. Environ. Implic. 1–25.
Tungsudjawong, K., Leungprasert, S., Peansawang, P., 2018. Investigation of humic acids concentration in different seasons in a raw water canal, Bangkok, Thailand. Water Sci. Technol. Water Supply 18, 1727–1738. https://doi.org/10.2166/ws.2017.235.
Usman, M., Ahmed, A., Yu, B., Wang, S., Shen, Y., Cong, H., 2021. Simultaneous adsorption of heavy metals and organic dyes by β-Cyclodextrin-Chitosan based cross-linked adsorbent. Carbohydr. Polym. 255. https://doi.org/10.1016/j.carbpol.2020.117486.
Wang, J. wei, Lan, Dai, Yong-qiang, Liu, Li, R. feng, Yang, X. ting, Lan, G. hong, Qiu, H. yan, Xu, B., 2021. Adsorption properties of β-cyclodextrin modified hydrogel for methylene blue. Carbohydr. Res. 501. https://doi.org/10.1016/j.carres.2021.108276.
Wang, Y., He, L., Dang, G., Li, H., Li, X., 2021. Polypyrrole-functionalized magnetic Bi2MoO6 nanocomposites as a fast, efficient and reusable adsorbent for removal of ketoprofen and indomethacin from aqueous solution. J. Colloid Interface Sci. 592, 51–65. https://doi.org/10.1016/j.jcis.2021.02.033.
Xia, D., Wang, P., Ji, X., Khashab, N.M., Sessler, J.L., Huang, F., 2020. Functional supramolecular polymeric networks: the marriage of covalent polymers and macrocycle-based host-guest interactions. Chem. Rev. 120, 6070–6123. https://doi.org/10.1021/acs.chemrev.9b00839.
Yang, A., Ching, C., Easler, M., Helbling, D.E., Dichtel, W.R., 2020. Cyclodextrin polymers with nitrogen-containing tripodal crosslinkers for efficient PFAS adsorption. ACS Mater. Lett. 2, 1240–1245. https://doi.org/10.1021/acsmaterialslett.0c00240.
Yang, C.A., Huang, H., Ji, T., Zhang, K.S., Yuan, L.Q., Zhou, C.S., Tang, K.W., Yi, J.M., Chen, X.B., 2019. A cost-effective crosslinked β-cyclodextrin polymer for the rapid and efficient removal of micropollutants from wastewater. Polym. Int. 68, 805–811. https://doi.org/10.1002/pi.5771.
Yi, Y., Tu, G., Zhao, D., Tsang, P.E., Fang, Z., 2019. Pyrolysis of different biomass pre-impregnated with steel pickling waste liquor to prepare magnetic biochars and their use for the degradation of metronidazole. Bioresour. Technol. 289, 121613 https://doi.org/10.1016/j.biortech.2019.121613.
Younis, S.A., Serp, P., Nassar, H.N., 2020. Jo ur n Pr. J. Hazard. Mater., 124562
Zhang, J., Li, M., Mao, H., 2019. Cross-linked enzyme aggregates of recombinant cyclodextrin glycosyltransferase for high-purity β-cyclodextrin production. J. Chem. Technol. Biotechnol. 94, 1528–1533. https://doi.org/10.1002/jctb.5912.
Zhang, X., Zhu, W., Guo, J., Song, J., Xiao, H., 2021. Impacts of degree of substitution of quaternary cellulose on the strength improvement of fiber networks. Int. J. Biol. Macromol. 181, 41–44. https://doi.org/10.1016/j.ijbiomac.2021.03.121.
Zhang, Xian, Zhang, P., Wu, Z., Pang, J., Zhang, Xianming, Li, Juan, Li, Jiding, 2020. Humic acid removal from water with PAC-AL30: effect of calcium and kaolin and the action mechanisms. ACS Omega 5, 16413–16420. https://doi.org/10.1021/acsomega.0c00532.
Zhang, Y., Liang, L., Chen, Y., Chen, X.M., Liu, Y., 2019. Construction and efficient dye adsorption of supramolecular hydrogels by cyclodextrin pseudorotaxane and clay. Soft Matter 15, 73–77. https://doi.org/10.1039/C8SM02203H.
Zhao, F., Repo, E., Yin, D., Meng, Y., Jafari, S., Sillanpää, M., 2015. EDTA-cross-linked β-cyclodextrin: an environmentally friendly bifunctional adsorbent for simultaneous

adsorption of metals and cationic dyes. Environ. Sci. Technol. 49, 10570–10580. https://doi.org/10.1021/acs.est.5b02227.
Zheng, X., Xu, T., Shi, R., Lu, N., Zhang, J., Jiang, C., Zhang, C., Zhou, J., 2018. Preparation of hollow porous molecularly imprinted polymers for N-nitrosamine adsorption. Mater. Lett. 211, 21–23. https://doi.org/10.1016/j.matlet.2017.09.047.
Zhong, C., 2020. Industrial-scale production and applications of bacterial cellulose. Front. Bioeng. Biotechnol. 8, 1–19. https://doi.org/10.3389/fbioe.2020.605374.